Neurotoxicity Research (2019) 36:563–582
https://doi.org/10.1007/s12640-019-00077-z

ORIGINAL ARTICLE

Age-Related Decrease in Tyrosine Hydroxylase Immunoreactivity in the Substantia Nigra and Region-Specific Changes in Microglia Morphology in HIV-1 Tg Rats

David R. Goulding[1] · Andrew Kraft[2,3] · Peter R. Mouton[4] · Christopher A. McPherson[2] · Valeria Avdoshina[5] · Italo Mocchetti[5] · G. Jean Harry[2]

Received: 26 March 2019 / Revised: 28 May 2019 / Accepted: 14 June 2019 / Published online: 8 July 2019

Abstract

Animal models have been used to study cellular processes related to human immunodeficiency virus-1 (HIV-1)-associated neurocognitive disorders (HAND). The HIV-1 transgenic (Tg) rat expresses HIV viral genes except the gag-pol replication genes and exhibits neuropathological features similar to HIV patients receiving combined antiretroviral therapy (cART). Using this rat, alterations in dopaminergic function have been demonstrated; however, the data for neuroinflammation and glial reactivity is conflicting. Differences in behavior, tyrosine hydroxylase (TH) immunoreactivity, neuroinflammation, and glia reactivity were assessed in HIV-1 Tg male rats. At 6 and 12 weeks of age, rotarod performance was diminished, motor activity was not altered, and active avoidance latency performance and memory were diminished in HIV-1 Tg rats. TH^+ immunoreactivity in the substantia nigra (SN) was decreased at 8 months but not at 2–5 months. At 5 months, astrocyte and microglia morphology was not altered in the cortex, hippocampus, or SN. In the striatum, astrocytes were unaltered, microglia displayed slightly thickened proximal processes, mRNA levels for *Iba1* and *Cd11b* were elevated, and interleukin (*Il*)1α,*Cxcr3*, and cell adhesion molecule, *Icam*, decreased. In the hippocampus, mRNA levels for *Tnfa* and *Cd11b* were slightly elevated. No changes were observed in the cortex or SN. The data support an age-related effect of HIV proteins upon the nigrostriatal dopaminergic system and suggest an early response of microglia in the terminal synaptic region with little evidence of an associated neuroinflammatory response across brain regions.

Keywords HAND · HIV · Rotarod · Dopamine · Microglia · Hippocampus · Astrocyte · Neuroinflammation · Learning

Introduction

Despite the introduction of combined antiretroviral therapy (cART), human immunodeficiency virus (HIV)-associated neurocognitive disorders (HAND) is present in the patient population (Letendre et al. 2010; McArthur et al. 2010; Heaton et al. 2010; Schouten et al. 2011). Compared with pre-cART, the differences reflect a shift from slowed motor function information processing to milder stages with effects on learning, memory, and executive function (Heaton et al. 2010; Schouten et al. 2011; Saylor et al. 2016; Sacktor and Robertson 2014), and a concern for adverse effects on brain structure and function remains (Gelman 2015; Chan et al. 2016; Boban et al. 2017; Clifford et al. 2017; Underwood et al. 2017; van den Dries et al. 2017; Sanford et al. 2018). In the pre- or naïve-cART HIV patient, CNS-associated disorders have been linked to changes in the dopaminergic system including, dopamine (DA) metabolism (Berger et al.

Electronic supplementary material The online version of this article (https://doi.org/10.1007/s12640-019-00077-z) contains supplementary material, which is available to authorized users.

✉ G. Jean Harry
harry@niehs.nih.gov

[1] Comparative Medicine Branch, National Institute of Environmental Health Sciences, Research Triangle Park, NC, USA

[2] National Toxicology Program Laboratory, National Institute of Environmental Health Sciences (NIEHS), P.O. Box 12233, MD E1-07, Research Triangle Park, NC 27709, USA

[3] Present address: U.S. Environmental Protection Agency Headquarters, Mail Code 8623R, William Jefferson Clinton Building, 1200 Pennsylvania Avenue, N. W, Washington, D.C. 20460, USA

[4] SRC Biosciences, Tampa, FL, USA

[5] Laboratory of Preclinical Neurobiology, Department of Neuroscience, Georgetown University, Washington, D.C., USA

1994), neuropathology in dopamine-rich brain regions (Kieburtz et al. 1991; Reyes et al. 1991; Lopez et al. 1999; Itoh et al. 2000; Gelman et al. 2006; Hu et al. 2009), reductions in substantia nigra (SN), tyrosine hydroxylase (TH), the enzyme responsible for catalyzing the conversion of the amino acid tyrosine to the dopamine precursor, L-DOPA (Silvers et al. 2006), and decreased dopamine transporter (DAT) levels in the putamen and ventral striatum (Wang et al. 2004). cART treatment in HIV patients appears to be insufficient in fully preventing such disruptions as reports of dopaminergic system dysfunction in this patient population continue (Kumar et al. 2009; Gaskill et al. 2017). The presence of viral proteins and possible exacerbation of dopaminergic system dysfunction has been suggested to contribute to neurocognitive disorders (Sheppard et al. 2015) and an association with Parkinsonism (DeVaughn et al. 2015). In addition, a role for neuroinflammation identified in pre-cART HAND appears to continue in cART era HAND (Gannon et al. 2011; Zayyad and Spudich 2015; Levine et al. 2016; Ginsberg et al. 2018), yet the association with cognitive deficits is not as well defined (Chen et al. 2014; Rao et al. 2014; Hong and Banks 2015). The observation that dopamine regulates a number of myeloid functions and that changes in DA concentration could influence myeloid function via DA receptor activation (Gaskill et al. 2012; Nolan et al. 2019) suggests a link between dopaminergic tone and neuroinflammation (Gaskill et al. 2013, 2014; Nolan et al. 2019). It is proposed that such chronic neuroinflammation may be tightly related to HAND comorbidities (Saylor et al. 2016; Vera et al. 2016). Information on the temporal and spatial associations between neuroinflammatory factors and the dopaminergic system will provide a better understanding of their role as contributing factors in the continued prevalence of HAND in the cART patient population.

While none of the available rodent models adequately replicate HIV patients under cART, they have been used to examine the potential association between HIV-related proteins and adverse nervous system outcomes, such as neuroinflammation, dopamine function, and learning and memory. Few have been used to examine the contribution of antiretroviral treatment which would more accurately reflect the cART patient population but may still have value as representative of a subgroup of the patient population. One model, the HIV-1 transgenic (Tg) rat, expresses all of the HIV viral genes, except the gag-pol replication genes, and proteins from birth, in the absence of actively replicating virus (Reid et al. 2001). This rat has been utilized to explore underlying biological processes associated with cART HAND (Reid et al. 2001; Vigorito et al. 2007; Lashomb et al. 2009; Lassiter et al. 2009; Peng et al. 2010; Royal III et al. 2012; Roscoe Jr et al. 2014) with the caveat that viral protein expression levels do not adequately reflect those in a cART patient. From the rodent studies, a number of processes have been implicated as important correlates, including synaptic simplification and injury (Atluri et al. 2013; Ru and Tang 2017), mitochondrial alterations (Rozzi et al. 2017), axonal transport (Avdoshina et al. 2016), and neuroinflammation (Repunte-Canonigo et al. 2014; Nesil et al. 2015; Sanna et al. 2017). The presence of HIV viral proteins alone damages DA neurons (Nosheny et al. 2006; Theodore et al. 2012; Miller et al. 2018), alters DA transporter (Webb et al. 2010; McIntosh et al. 2015; Bertrand et al. 2018), mediates striatal dopaminergic synapses (Sinharay et al. 2017), facilitates synaptic loss (Kim et al. 2011; Shin et al. 2012), and alters dendritic spines of medium spiny neurons and DA uptake in the striatum (Javadi-Paydar et al. 2017). Diminished immunostaining in the striatum for TH suggested an enzymatic deficit in dopaminergic projections from the SN (Reid et al. 2016a). Such changes in dopamine function have been reflected in behavioral alterations in HIV-1 Tg rats (Liu et al. 2009; Moran et al. 2013; Zhu et al. 2016; Javadi-Paydar et al. 2017). While susceptibility of the dopaminergic system continues to gain support, questions remain as to the mechanism by which this occurs given that neurons are not infected by the virus. An alternative mechanism proposed is that infected microglia are a source of viral proteins or inflammatory factors that, upon release, can damage neurons. While neuroinflammation has been implicated in HIV-1 Tg rats, the findings are inconsistent (Table 1), making it difficult to identify a relationship with behavioral or dopaminergic alterations.

Overall, studies report an absence of neuronal death in HIV-1 Tg rats. However, one recent study reported hippocampal neuronal loss and an associated glia response to injury (Cho et al. 2017). With the exception of the Cho et al. (2017) study, only subtle changes in microglia and astrocytes have been observed, with no clear pattern of an association with elevations in proinflammatory related factors. For example, Repunte-Canonigo et al. (2014) reported an increase in microglia number in the hippocampus and cortex but changes in related genes occurred only in the hippocampus. Further observations of a morphological response of glia in the absence of an associated proinflammatory response were provided by Reid et al. (2016a), and Rowson et al. (2016) reported mild morphological differences in microglia with a slight elevation in complement factor b (*Cfb*) but no measurement of proinflammatory factors. Using translocator protein TSPO imaging and mRNA levels of proinflammatory cytokines, Lee et al. (2015) reported no evidence of inflammation in the cortex, hippocampus, or striatum of 9-month-old HIV-1 Tg rats. The conflicting and less than robust reports raise doubts with regard to an early contribution of neuroinflammation and suggest alternative functions for the few morphological changes observed in microglia and astrocytes.

The current study was undertaken to evaluate alterations in HIV-1 Tg rats across a number of related factors. Rotarod performance and motor activity were conducted to evaluate

Table 1 Summary of publications on neuroinflammation, glial response, and behavior in HIV-1 Tg rat brain regions

Author	Sex	Age	mRNA		Proteins		Histochemistry		Imaging		Behavior	
Avdoshina et al. 2017	M	5 months	CTX ($n = 4$)		CTX ($n = 4$)		CTX ($n = 4$)					
F344/NHsd			*Il1b*	nc	Ac-tubulin	dec	iba1	nc				
			Tnfa	nc								
Blanchard et al. 2015	M	9 months			HEMIS ($n = 10$; 12)							
F344/NHsd					PGE2	in						
					8-Isoprostane	in						
					15-Epi-LXA4	in						
					TXB2	nc						
					15-HETE	nc						
					LTB4	nc						
					LXA4	nc						
Chivero et al. 2017	M/F	18 months	STR ($n = 4$)		STR ($n = 4$)							
			Il1b	in	IL-1β (17 kDa)	in						
			Il6	in	ASC	in						
					Caspase 1	in						
Cho et al. 2017	ns	5 months			HIPP ($n = 4$)		HIPP ($n = 4$)					
F344/NHsd					AC3	in	H&E	Cell death				
					Bax	in	Cresyl violet	Cell death				
					NeuN	dec	AC3	in				
					GFAP	in	GFAP	in				
					C99	in	NeuN	in				
					β-Amyloid	in	Congo red	in				
					p-Thr181	in	Beta amyloid	in				
					p-Thr231	in	CTX ($n = 4$)					
					p-Ser396	in	NeuN	dc				
					TNF-α	in	GFAP	dc				
					MCP-1	in						
Guo et al. 2012	ns	3–6 months					CA1 HIPP					
F344/NHsd							NeuN	nc				
							Parvalbumin	nc				
Lee et al. 2015	M	3–16 months			Brain slice		Iba1 number		[18F]DPA-714 PET			
F344/NHsd					CTX, HIPP, STR		1–10 months ($n = 14$; 12)		3 months ($n = 4$; 4)	nc		
					24-plex assay		CTX	nc	9 months ($n = 5$; 5)	nc		
					3 months ($n = 5$; 5)	nc	HIPP	nc	16 months ($n = 3$; 6)	nc		
					9 months ($n = 4$; 5)	nc	STR	nc				
Nemeth et al. 2014	F	48 days	HIPP ($n = 10$; 9)				HIPP ($n = 9$; 12)				Motor function	nc
F344/NHsd			*Ccl2*	in			Ki-67	dec			Open-field (10 min)	nc
			Tnf	nc							Startle	nc
			Il1b	nc							Sucrose preference	nc
			Nfxbia	nc							Forced swim	nc
											Social behavior	dec
Pang and Panee 2016	ns	10 months	HIPP ($n = 5$)		HIPP ($n = 5$)							

Table 1 (continued)

Author	Sex	Age	mRNA		Proteins		Histochemistry		Imaging		Behavior	
HIV-1 NL4–3			*Gfap*	nc	GFAP	in						
gag-pol Tg			*Iba1*	nc	Iba1	dec						
			Tnfa	nc	IL-1b	in						
			Il1b	in	NFκB p65	nc						
					c-Jun	in						
Reid et al. 2016b									18F-FDG uptake		Rotarod ($n = 4$; 5)	
F344/NHsd									4–31 weeks ($n = 4$)	nc	4–7 weeks	dec
									12 weeks ($n = 5$)	nc	8–20 weeks	nc
									29 weeks ($n = 4$; 5)	nc	Open-field ($n = 4$–5)	
									14C-DG		11–25 weeks	dec
									7–8 months ($n = 5$)	nc		
Reid et al. 2016a	M	1–20 months	1 month ($n = 3$)				1 and 3 months ($n = 6$; 8)					
F344/NHsd			8–9 months ($n = 5$)				7 and 9 months ($n = 7$; 9)	NeuN/GFAP				
			STR/HIPP				STR	dec/dec				
			Gfap	nc			HIPP	nc/dec				
			Iba1	nc			CTX	nc/dec				
			Cd11b	nc				Iba-1 number				
							STR/HIPP/CTX	nc				
Repunte-Canonigo et al. 2014	ns	4–5 months	HIPP ($n = 6$; 5)				HIPP, CTX ($n = 5$)	Intensity/no.			T maze ($n = 7$)	
SD			*Gfap*	in			GFAP	in/in			Spontaneous alternation	dec
			Iba1	in			Iba-1	in/in			latency	nc
			Cd11b	in								
			INF signaling	in								
			Cell division	in								
Rowson et al. 2016	M/F	54 days	HIPP				HIPP ($n = 3$)					
F344/NHsd			*Cfb*	in			Iba-1					
			Lcn2	nc			No. of branches	in				
			PFC				No. of junctions	in				
			Cfb	dec			Max branch length	in				
			Lcn2	dec			Avg. branch length	nc			Novel object	
							RECA-1				M ($n = 8$; 9)	dec
							PFC ($n = 3$; 5)	nc			*F* ($n = 9$; 7)	dec
							Amygdala ($n = 5$;6)	nc				
							HIPP ($n = 5$;6)	nc				
Royal et al. 2012	ns	ns			HEMIS ($n = 2$)		Brain ($n = 2$)	Area/intensity				
F344/NHsd					IFN-γ	in	GFAP	nc/nc				
					TNF-α	in	MHC ii	in/in				
					IL-1β	in	ED-1	in/in				
							Iba-1	in/in				
Yang et al. 2016	M	3 months	mRNA		mRNA		mRNA					
F344/NHsd			NAac		PFC		VTA					
			Casp3	in	*Casp1*	dec	*Casp3*	in				
			Cx3c11	in	*Ccl5*	dec	*Cx3cr1*	in				
			LRF4	in	*Tgfb*	dec	*Il1b*	in				

Table 1 (continued)

Author	Sex	Age	mRNA		Proteins		Histochemistry		Imaging	Behavior
			Irf7	in	*TLR4*		*Il1b*	dec		
			Ccl5	dec						
			Cx3cr1	dec						
			Il1a	dec						
			Tgfb1	dec						
			Tlr4	dec						

M male, *F* female, *CTX* cortex, *HEMIS* brain hemisphere, *HIPP* hippocampus, *NAc* nucleus accumbens, *PFC* prefrontal cortex, *STR* striatum, *VTA* ventral tegmental area

motor related deficits and compare with the literature and learning and memory was assessed using an active avoidance paradigm. TH immunoreactivity in the SN was examined across ages to examine alterations in dopaminergic neurons to compare with changes in TH immunoreactivity observed in the striatum of HIV-1 Tg rats (Reid et al. 2016a) and SN of GT-tg bigenic mice (Miller et al. 2018). Morphological alterations in astrocytes and microglia and mRNA levels for inflammatory factors were examined in specific brain regions previously reported. It is our expectation, that while descriptive, the collation of these endpoints across ages and in the same animal will help to set the framework to more fully describe the relationship. Such information will facilitate our ability to fully utilize this experimental model to address relevant biological and therapeutic questions as they may apply to the human patient population.

Materials and Methods

Animals

Male HIV-1 transgenic rats (Fischer 344/NHsd; Tg) and Fischer 344 (F344) rats were obtained from Harlan Laboratories (Madison, WI). All HIV-1 Tg rats displayed cataracts. Male rats were examined as based upon the predominance of data from male rats, or unspecified sex distributions, in the existing literature on neuroinflammation in HIV-1 Tg rats. Rats were assessed across multiple cohorts and randomly assigned to endpoints and age of analysis. Animals were housed within an Association for Assessment and Accreditation of Laboratory Animal Care accredited facility (40–60% humidity; 12-h light/dark cycle 6:00–18:00 EST; 20–24 °C) under isolator housing conditions to minimize any possibility of nonspecific immune challenge. Rats were allowed ad libitum access to reverse osmosis deionized drinking water and maintained on their Harland Labs original diet (Teklad Global 18% protein 2018S diet; Teklad Harlan, Madison, WI; sterilized for controls and gamma-irradiated for HIV-1 Tg rats to minimize risk of infection). The diet contained (as % of total fatty acid) 16.7% saturated, 21.8% monounsaturated, 54.8% linoleic acid, 6.2% α-linolenic acid, 0.03% AA, 0.02% eicosapentaenoic acid (EPA, 20:5 n-3), and 0.06% docosahexaenoic acid (DHA, 22:6). Animal studies were done in accordance with the National Institutes of Health *Guide for the Care and Use of Laboratory Animals* following approved animal protocols from the Animal Care and Use Committee of the National Institute of Environmental Health Sciences.

Behavioral Assessments

Behavioral assessments of motor function used test systems similar to those in the literature, and learning and memory was evaluated within each of these tests and with a nonvisually dependent task of active avoidance. Assessments were conducted at ages prior to overt evidence of immunohistological changes in the SN. Handling and husbandry of rats for behavioral testing followed the National Toxicology Program (NTP) guidelines for neurobehavioral testing (NTP 2015). Rats were transported to animal facility holding area 1 h prior to testing to allow for acclimation. All testing was conducted between 10:00 and 15:00 h. Assignment to testing chamber and to time of testing was counterbalanced, and animals were assessed under experimenter-blinded conditions.

Rotarod One of the more consistent effects reported in the HIV-1 Tg rat is a deficit in rotarod performance (June et al. 2009; Reid et al. 2016b) and thus was included with assessment at 6 weeks ($n = 18$), 12 weeks (F344 $n = 14$; HIV-1 Tg = 17), and 24 weeks ($n = 7$) of age to compare our findings to those reported in the literature. Performance on an accelerating rotarod was evaluated using a Rotamex-5 (Columbus Instruments, Columbus, OH) equipped with the rat spindle (7 cm × 9.5 cm). Rats were placed on the stationary spindle and rotations initiated at acceleration increments of 1 rpm/10 s. Rats were allowed two initial training trials followed by a sequence of 6 trials with an intertrial interval (ITI) of 30 min. Latency for remaining on the rotating rod, as automatically photocell-detected, was recorded with a maximum time of 5 min allowed for each trial. At 8 months of age, the weight and size of the rats were such that the rat spindle was not of sufficient size to allow the rats to perform the task, and thus, all rats fell within the first few rotations, and the task did not provide a valid assessment. This data is therefore not provided.

Motor Activity Motor activity has been previously reported to be diminished in adult male HIV-1 Tg rats 11–25 weeks of age (Reid et al. 2016b). Adult rats (24 weeks of age; $n = 10$) were assessed for exploratory ambulatory activity in a novel environment. Activity was recorded in 5-min epochs over 30 min in an OptoMax Activity photocell device (42 cm × 42 cm × 20 cm; Columbus Instruments, Columbus, OH) under dim-light conditions. Ambulatory activity, time spent within the margin of the arena, and distance traveled in the margin zone of the arena were recorded.

Active Avoidance As a measure of learning and memory, rats were sequentially examined at 6 ($n = 8$), 12 ($n = 8$), and 24 weeks ($n = 7$) for performance in an active avoidance procedure. Animals were placed into one compartment of the shuttle box (Gemini II shuttle box, San Diego Instruments, San Diego, CA), the guillotine door was opened, and a 2-min general exploratory period was initiated. The session was initiated with the delivery of a cue light and tone (conditioned stimulus, CS) on the side of the apparatus containing the rat. The CS was delivered 10 s prior to and continued throughout the delivery of a 10-s 0.6-mA scrambled foot shock (unconditioned stimulus; US), resulting in a 20-s response period. Movement of the rat to the "safe" side terminated the CS and US. A total of 60 CS/US pairings were delivered within a session on a 15-s variable ITI schedule. Avoidance responses and latency were recorded for the animal moving to the "safe" side during the 10-s interval between CS and US. Escape responses were recorded for shifting to the "safe" side during the US delivery. Mean responses were calculated for each 10-trial unit for a total of 6 units representing 60 trials.

Tissue Collection for Histology

Rats were euthanized with isofluorane, whole body cardiac perfused with saline, decapitated and the brain rapidly excised, cut in the midsagittal plane, and one hemisphere immersion-fixed in 4% paraformaldehyde/phosphate buffer (pH 7.2) for 18 h, rinsed, and placed in FD Tissue Cyroprotection Solutions (FD NeuroTechnologies, Inc., Columbia, MD). Samples were maintained at − 20 °C until sectioning. Cyroprotected brain hemispheres were shipped to FD NeuroTechnologies (Ellicott City, MD) for sectioning and immunostaining. Forty-micrometer free-floating coronal serial cryosections (every 1st–10th section of each series of 10 sections with an interval of 400 μm between 3.00 and − 7.04 mm Bregma) were collected and stored in cryoprotection solution (FD NeuroTechnologies, Baltimore, MD) at − 20 °C. For comparison to the existing literature, morphology of microglia and astrocytes was examined in the hippocampus, cortex, striatum, and SN.

Unbiased Stereology for TH^+ Neurons in SN

To determine if TH immunoreactivity was diminished in neurons of the SN/VTA, unbiased stereological analysis was conducted. Systematic random samples of 40-μm serial sections through the SN_{PC}-VTA were collected between Bregma − 4.36 and − 7.04 mm with an interval of 120 μm. Sections were washed with 1X Tris-buffered saline (TBS; Quality Biological, Inc., Gaithersburg, MD) and endogenous peroxidases quenched by 1% hydrogen peroxide for 30 min at RT, followed by rinses with 1X TBS and incubation with 0.3% Triton X. Sections were blocked with 5% normal goat serum in 1X TBS and then incubated with 1:2000 rabbit antityrosine hydroxylase (Santa Cruz Biotechnology, Dallas, TX) overnight at 4 °C. Following primary incubation, sections were rinsed with 1X TBS and incubated in biotinylated anti-rabbit

secondary antibody (1:400; Vector Laboratories, Burlingame, CA) with normal goat serum in 1X TBS for 90 min at RT. Rinsed sections were incubated using Vectastain Elite ABC Kit for 90 min at RT, washed in 1X TBS, and treated with 3-diaminobenzidine (DAB; Agilent Technologies, Santa Clara, CA) (10 mg DAB in 40 ml 1X TBS) and chromogen with nickel chloride amplification. Sections were mounted on poly-L lysine-coated slides and coverslipped.

Total number of TH^+ neurons in the SN reference space was quantified using the optical fractionator method and the *Stereologer* system (Stereology Resource Center, Chester, MD), as previously reported (Mouton et al. 2002; Marcario et al. 2004; Mouton and Gordon 2010). The reference space was outlined under low magnification (× 5) for each section, and TH^+ neurons counted at high magnification (× 63 oil immersion), with a guard volume of 2 μm. For counts of total neuron number, the following sampling fractions were used: section sampling fraction (ssf, number of sections sampled divided by the total number of sections); area sampling fraction (asf, area of the sampling frame divided by the area of the *x-y* sampling step); and thickness sampling fraction (tsf, height of the dissector divided by the section thickness). The counting criteria were TH immunoreactivity in the cytoplasm of cells with a neuronal phenotype, including a clear nuclear membrane and distinct nucleolus. Sampling of *x-y* locations was continued to a high level of sampling stringency, i.e., 0.10 to 0.15 mean coefficient of error (CE, Gundersen et al. 1999) per group.

Immunostaining for Glial Fibrillary Acidic Protein and Ionized Calcium-Binding Adapter 1

Sections containing the SN (− 4.0 to − 7.0 from Bregma), striatum (− 2.6 to − 1.0 mm from Bregma), and hippocampus (− 3.0 to − 4.5 from Bregma) were washed with phosphate-buffered saline (PBS), equilibrated to room temperature (RT), and incubated for 2 h in a blocking solution containing 2% goat serum, 1% bovine serum albumin, and 0.1% Triton X-100 in automation buffer (Biomedia, Foster City, CA). Sections were incubated with anti-GFAP (1:200, Dako Agilent Technologies, Carpinteria, CA) or anti-Iba-1 (1:500, Wako Chemicals, Richmond, VA) in blocking solution (18 h; 4 °C), reequilibrated to RT. Rinsed sections were incubated using Vectastain Elite ABC Kit and visualized by DAB. Sections used for immunofluorescence were incubated with Alexa Fluor antibody conjugates (594 nm or 488 nm; 1:250, Invitrogen Thermo Fisher, Carlsbad, CA) in blocking solution without Triton X-100 (2 h; RT), mounted on charged slides in Prolong with DAPI (Invitrogen, Thermo Fisher), and coverslipped.

Digital images of immunostaining were collected using a LSM 410 inverted confocal laser scanning microscope (Carl Zeiss, Oberkochen, Germany). For acquisition, the pinhole diameter, scan speed, and amplifier gain were kept constant. The detector gain and amplifier offset were determined from the range indicator function in Fast XY mode. Image stacks were collected through the full depth of the tissue. At × 20 magnification, 1.5-μm steps were collected with a 2048 × 2048 frame size; at × 63 magnification, 1.0-μm steps were collected with a frame size of 1728 × 1728. Stacks were displayed as a single image using 3D maximum projection. DAB sections were scanned under × 20 magnification (Aperio ScanScope T2 scanner, Aperio Technologies, Inc., Vista, CA), image stitched, and viewed using Aperio ImageScope v.6.25.0.1117. Stained slides were assigned random numbers and blinded for evaluation. Defined regions of interest (ROI) in the hippocampal dentate gyrus, motor cortex, striatum, and SN were evaluated for overt changes in astrocyte or microglia morphology and any evidence of neuronal loss. The scoring system for morphology (20 cells/2 sections/rat) was based on previously published work and reflected the different morphological features observed within each region (Heppner et al. 1998; Kanaan et al. 2008; Harry et al. 2014). Observations of a thickened proximal process of microglia in the striatum were confirmed using ImageJ 1.48v (National Institutes of Health) with the width of the cell body and the proximal process calculated for a minimum of 20 cells within the ROI for each section. For the hippocampus and cortex, images of Iba-1 immunohistochemical (DAB) sections were analyzed using contrast that was optimized within the green channel grayscale images, and the threshold was set to a lower level of 0 and an upper level between 175 and 185. This range allowed for inclusion of all Iba-1^+ microglia within the image plane. The area fraction occupied by Iba-1^+ cells was calculated using the measurement tool and expressed as percent total area.

qRT-PCR for Inflammatory Factors

From the contralateral hemisphere to that used for histology, the striatum, motor cortex, and hippocampus were dissected. Under a dissection microscopy, an area enriched for the SN/VTA was micropunched from the relevant brain slice obtained using a brain matrix. Samples were stored at − 80 °C. Total RNA was extracted using TRIzol Reagent (Invitrogen, Thermo Fisher). RNA quantity and purity were assessed using NanoDrop (Thermos Scientific, Wilmington, DE), and complementary deoxyribonucleic acid (cDNA) was synthesized from 2.5 μg total RNA using SuperScript™ II reverse transcriptase with random hexamers (Invitrogen, Thermo Fisher). qPCR was performed in duplicate using 2.5 μl cDNA as a template in combination with Power SYBR Green Master Mix (Applied Biosystems, Foster City, CA) and optimized forward and reverse primers (Supplementary Table 1). The reaction mixtures were held at 50 °C for 2 min and 95 °C for 10 min, followed by 40 cycles at 95 °C for 15 s and 1 min at 60 °C. Amplification curves were generated with

sequence detection system 1.9.1 software (Applied Biosystems). Threshold cycle values were determined, and the mean fold changes over age-matched WT controls were calculated according to the $2^{\Delta\Delta CT}$ method and normalized to housekeeping gene. For all primers, a melting curve analysis was performed by denaturation at 95 °C for 15 s, annealing at 60 °C for 1 min at a melting rate of 0.3 °C/s to 95 °C. Each qRT-PCR was carried out in sample duplicates and replicated with two different housekeeping genes, glyceraldehyde 3-phosphate dehydrogenase (GAPDH) and cyclophilin, by different investigators. Data were obtained from samples that met inclusion criteria of transcript detection at $\leq$ 32 PCR cycles.

Statistical Analysis

Statistical analyses were performed using GraphPad Prism software (GraphPad Software, Inc., San Diego, CA). Levene's test was used to test for homogeneity of variance. Rotarod, motor activity, and active avoidance at each age were

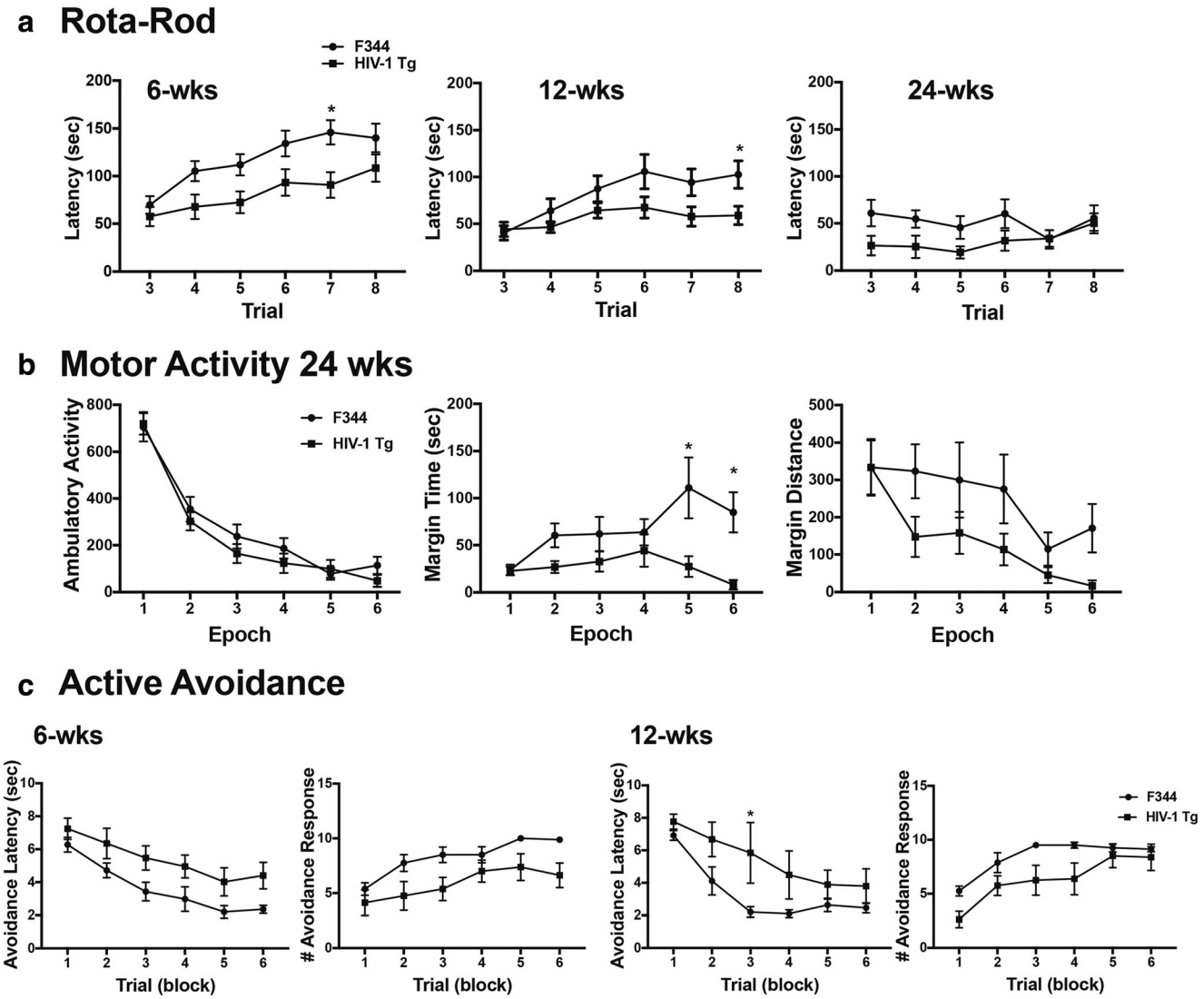

Fig. 1 **a** Accelerating rotarod. Latency to fall from a rotarod was determined across 6 trials (3–8), following 2 training trials, in F344 and HIV-1 Tg male rats at 6 ($n = 18$), 12 (F344 $n = 14$; HIV-1 Tg $n = 17$), and 24 weeks of age ($n = 7$). Performance increased over successive trials at 6 and 12 weeks of age ($p < 0.0001$). HIV-1 Tg showed significantly overall shorter latencies at 6 ($p < 0.01$) and 12 weeks ($p < 0.05$) but not at 24 weeks. **b** Open-field activity in 5-month-old rats ($n = 10$). Activity significantly decreased over the session ($p < 0.0001$) in both groups. Time spent within the margin was significantly less in the HIV-1 Tg rats ($p < 0.05$). No difference was observed for distance traveled in the margin. **c** Shuttle box active avoidance at 6 and 12 weeks of age. Avoidance latency (sec) and no. of avoidance responses occurring over 6 blocks of 10 trials each. At 6 and 12 weeks of age ($n = 8$), rats showed acquisition of the task in latency ($p < 0.0001$) and no. of avoidance responses ($p < 0.0001$). At both ages, HIV-1 Tg rats displayed longer latencies ($p < 0.05$) and lower no. of avoidance responses ($p < 0.05$). At 12 weeks, the latency response pattern for HIV-1 Tg rats was similar to that observed on training at 6 weeks while F344 reached performance plateau by trial block 3. Data represents mean ± SEM. *$p < 0.05$

analyzed by repeated measures ANOVA (RM ANOVA) with genetic background and epoch/trial as the main factors. Sidak's multiple comparison test was used to examine differences at individual trial blocks. Unbiased stereology data and imaging density data were analyzed by Student's *t* test as each age assessment was conducted in independent groups of rats. Rating scale for microglia morphology in the striatum was calculated as percentage of total microglia within the ROI and analyzed by the Mann-Whitney *U* test. Thickness of microglia processes was analyzed by Student's *t* test. A maximum of 5 endpoints for qPCR were assessed in any one independent group of RT samples. Student's *t* tests were conducted with brain region considered as an independent factor given that, while from the same rat, the samples were experimentally handled as independent. To address issues of experiment-wise error rate, statistical analysis of mRNA was conducted on transcripts that showed a minimum of a 20% difference. False discovery rate was determined using the Benjamini-Hochberg (BH) procedure. The order of analysis for transcripts was maintained across regions, and any BH corrections are noted in the text. Statistical significance was set at $p < 0.05$. Results are expressed as mean ± standard deviation or standard error as indicated.

Results

Behavioral Testing

Behavioral assessments of motor coordination were conducted at 6, 12, and 24 weeks of age, allowing for a comparison with a clear reproducible effect reported in the literature. Learning and memory were assessed using a shock-based active avoidance procedure at 6 and 12 weeks of age. Motor activity was assessed at 24 weeks of age for comparison with findings in the literature. As noted in the "Materials and Methods" section, the size and weight of rats the older ages presented issues with assessing behavior in these tasks.

Rotarod Performance on the accelerating rotarod represents primarily motor strength and coordination but can also reflect task-specific learning as indicated by an increase in performance with training. Consistent with previous reported deficits in motor strength and coordination in HIV-1 Tg rats (June et al. 2009; Reid et al. 2016b), an overall deficit in rotarod performance was observed in HIV-1 Tg rats (Fig. 1a). Over age, performance in all rats declined (Reid et al. 2016b). At 6 weeks of age, latency to fall over trial was significantly shorter in HIV-1 Tg rats as compared with F344 rats ($F_{(1,34)} = 11.12$; $p = 0.0021$). However, both F344 and HIV-1 Tg rats showed a similar increase in performance over successive trials ($F_{(5,170)} = 9.275$, $p < 0.0001$). At 12 weeks of age, all rats showed slightly lower latencies than that observed at 6 weeks of age (Fig. 1a). Over the session, HIV-1 Tg rats displayed significantly shorter latencies to fall as compared with F344 rats ($F_{(1,29)} = 5.69$, $p = 0.0238$). Yet, an increase in performance over successive trials was observed in both groups ($F_{(5,145)} = 6.718$, $p < 0.0001$), with no evidence of a significant interaction between trial and genotype. At 24 weeks of age, all rats showed shorter latencies to fall as compared with younger ages but also failed to show betterment in performance over trials (Fig. 1a). No difference was observed between groups; however, this absence of differences was likely related more to the overall age and animal size-related decrease in performance rather than genetic differences. The overall age-related decrease in performance seen between 6 and 24 weeks of age across all animals and the performance deficit observed in HIV-1 Tg rats are consistent with findings reported by Reid et al. (2016b). They do, however, raise questions with any interpretation of data obtained from the older, larger rats.

Motor Activity Ambulatory activity within the open field provides an assessment of exploratory activity and is often considered to reflect a dopaminergic-related motor behavior. In 20-week-old rats, total ambulatory activity was similar between groups (Fig. 1b). A normal pattern of activity was observed and characterized by a progressive decrease in activity over the session across 5-min epochs ($F_{(5,90)} = 85.22$, $p < 0.0001$) with no significant differences observed between F344 and HIV-1 Tg rats. The absence of any difference in ambulatory activity at this age is consistent with findings of Reid et al. (2016b). The test paradigm however is somewhat different in that motor activity that was assessed over 2-week intervals in the Reid et al. (2016b) study, thus acclimating the rats with the open-field environment no longer having characteristics of a novel environment towards the end of assessment. As compared with the analysis of total session activity levels in the Reid et al. (2016b) study, the current study examined the response of rats naïve to the novel open-field environment and examined activity over time epochs to examine habituation. A normal pattern of activity was observed in both groups, characterized by a progressive decrease in activity over 5-min epochs ($F_{(5,90)} = 85.22$, $p < 0.0001$), suggestive of normal response and habituation to a novel environment. Based on a previous report that HIV-1 Tg rats display a greater "anxiety-like" response (Reid et al. 2016b), ambulatory activity localized to the margin, thigmotaxis, was recorded (Fig. 1b). Consistent with the decrease in overall activity levels across epochs, activity in the margin decreased over the session in both groups (time spent: $F_{(5,90)} = 3.37$, $p = 0.0191$; distance traveled: $F_{(5,90)} = 8.483$, $p < 0.0001$). In contrast to Reid et al. (2016b), total time spent within the margin zone ($F_{(1,18)} = 6.621$, $p < 0.05$) was less in HIV-1 rats while no difference was observed for total distance traveled ($p < 0.1$).

F344 rats showed an increase in time in the margin during the 5th and 6th epoch that was not observed in the HIV-1 Tg rats ($p < 0.05$). The difference in margin time was not related to differences in overall activity levels of the rats. Thus, at this age, we observed no evidence of "anxiety-like" behavior with regard to preference for the margin region.

Active Avoidance In the active avoidance task, rats were required to learn an association between the conditioned stimulus (CS: i.e., light/tone) and the delivery of the unconditional stimulus (US: i.e., foot shock) to respond in a manner to avoid receiving the shock. As training proceeds, animals learn to avoid the US by shuttling across a divided chamber during the CS. This crossing terminates the tone and prevents receipt of the shock. Signaling for active avoidance requires an intact flow of information between the basal amygdala and the shell region of the nucleus accumbens (Ramirez et al. 2015) and possibly requires suppression of the amygdala-mediated defensive reactions by the prefrontal cortex (Moscarello and LeDoux 2013). At 6 weeks of age, all rats showed a significant decrease in avoidance latency to respond to the CS over session trials ($F_{(5,70)} = 13.25$, $p < 0.0001$), indicative of learning (Fig. 1c). However, significant overall longer avoidance latencies across trials were observed in HIV-1 Tg rats as compared with F344 rats ($F_{(1,14)} = 8.322$, $p = 0.012$) with no significant interaction observed between trials and genetic background. Avoidance performance (no. of avoidance responses) significantly improved over the session ($F_{(5,70)} = 7.983$, $p < 0.0001$) for both groups; again suggestive of learning, however, a deficit was suggested with the significantly less no. of avoidance responses in the HIV-1 Tg rats as compared with F344 rats ($F_{(1,14)} = 7.853$, $p < 0.05$) (Fig. 1b). By 12 weeks of age, a progressive decrease in avoidance latency over trials was observed for both groups ($F_{(5,70)} = 16.68$, $p < 0.0001$; Fig. 1c). HIV-1 Tg rats showed a higher overall avoidance latency, similar to that seen at 6 weeks and, while

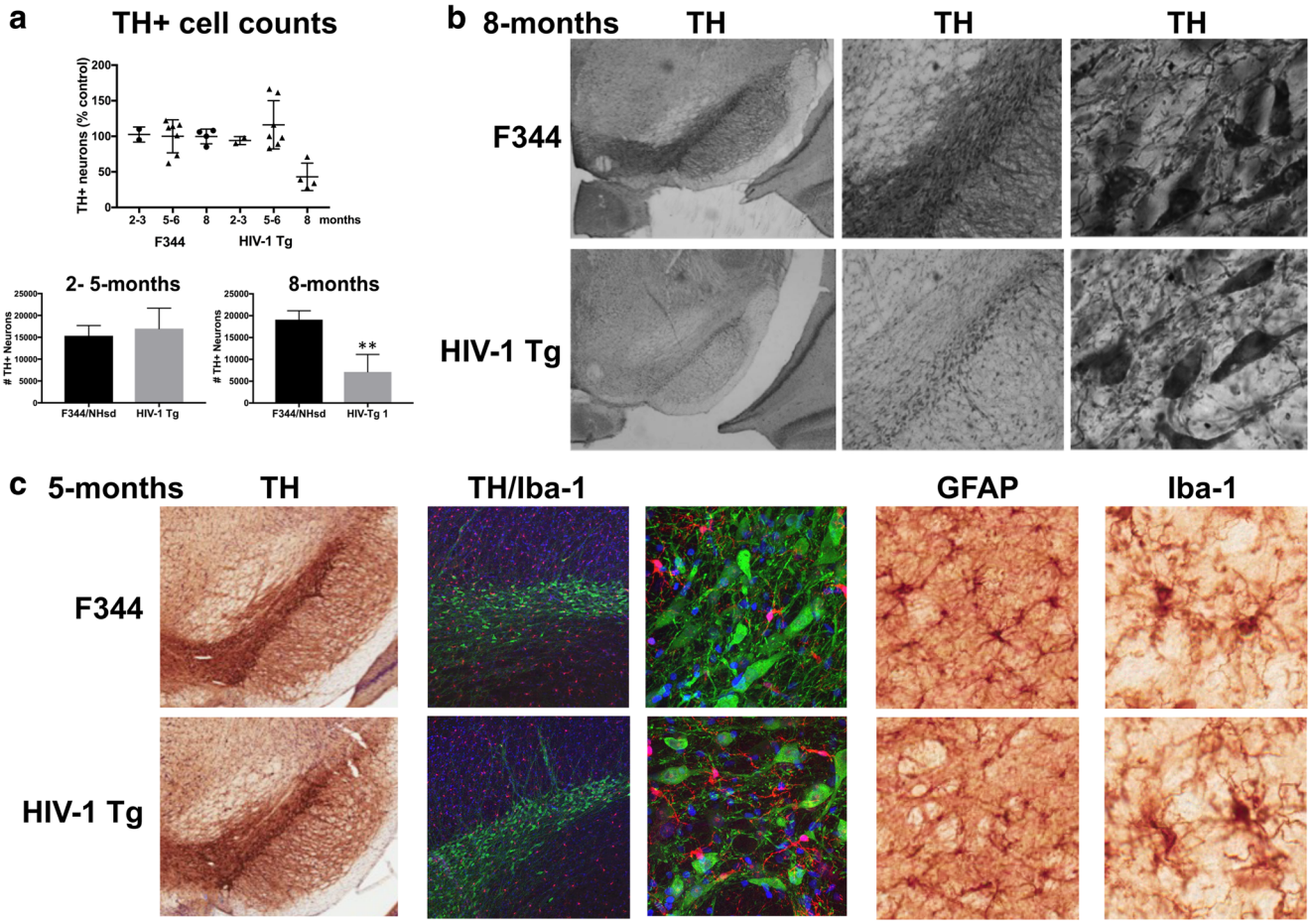

Fig. 2 Tyrosine hydroxylase immunoreactivity and unbiased stereology. **a** Estimates of TH^+ neuronal number between 2 and 8 months of age. Scatter graph of individual values (% of F344 control) at each age. Bar graphs of mean ± SEM for 2–5 months ($n = 9$) and 8 months ($n = 4$–5). No difference was observed between 2 and 5 months of age. At 8 months of age, HIV-1 Tg rats showed significantly fewer TH^+ neurons as compared with age-matched controls ($p = 0.002$; $n = 4$–5). **b** TH immunoreactivity (3,3-diaminobenzidine staining: brown, black) in the SN at 8 months of age. **c** At 5 months of age, TH immunoreactivity in the SN showed no difference between F344 and HIV-1 rats with DAB staining or fluorescence (green) staining. Iba-1^+ microglia showed similar morphology across groups as shown by immunostaining for Iba-1 (red, DAB). GFAP staining (DAB) showed no difference between groups

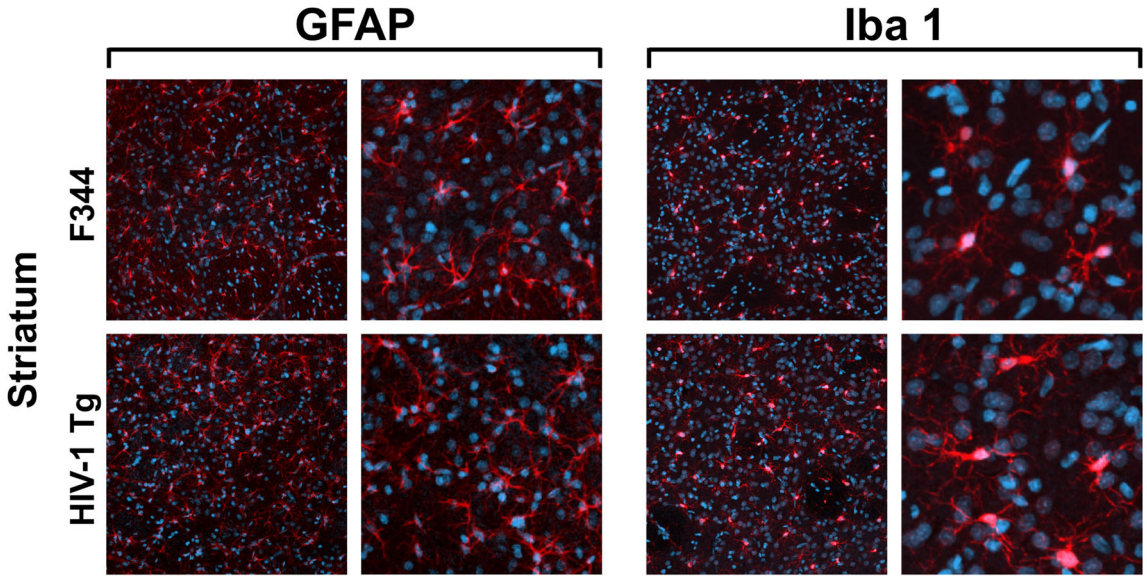

Fig. 3 Immunoreactivity for GFAP and Iba-1. Representative images of GFAP$^+$ astrocytes and Iba-1$^+$ microglia in the striatum of F344 and HIV-1 Tg 5-month-old male rats. Immunofluorescent staining for GFAP (red) with DAPI (blue) counterstain showed astrocytes with elongated thin processes in F344 and HIV-1 Tg rats with no evidence of astrocyte hypertrophy. Iba-1$^+$ microglia (red) were characterized as thin process-bearing cells in F344 rats. In HIV-1 Tg rats, microglia were similar but displayed slightly thickened proximal processes

the overall differences across trials failed to reach statistical significance ($p = 0.08$). F344 rats show improved performance by the 2nd and 3rd trial as compared with the HIV-1 Tg rats, suggestive of a memory deficit. The no. of avoidance responses significantly increased over trials for both groups ($F_{(5,70)} = 15.24$, $p < 0.0001$; Fig. 1b). HIV-1 Tg rats showed overall significantly lower no. of avoidance responses ($F_{(1,14)} = 5.242$, $p < 0.05$) reaching a maximum level by trial block 5 as compared with trial block 3 in the F344 suggestive slight effect on memory. At 24 weeks of age, rats had progressed to a body size and weight that significantly limited their ability to transgress through the door connecting the two chambers. This resulted in significantly lower avoidance responses (2–3) and longer latencies (8–10 s) in both groups, and by the 3rd trial block of the session, all responses were "escape losses" with the rats adopting a freezing behavior. Sessions were terminated at the end of the 3rd trial block. Data is not reported.

TH Immunohistochemistry and Unbiased Stereology in the SN

TH expression in the SN is considered to reflect dopaminergic neuronal integrity. Thus, we examined TH staining to reveal whether HIV-1 Tg rats exhibited alterations of the dopaminergic system. By 8 months of age, a significant decrease in TH$^+$ immunoreactive neurons was observed in HIV-1 Tg rats as compared with age-matched F344 rats ($t = 5.198$, $p = 0.002$; Fig. 2a). As HIV-1 Tg rats constitutively express HIV viral proteins throughout development, TH$^+$ immunoreactivity was examined at earlier ages to determine if the changes were developmentally present or if they represented a loss over time. Between 2 and 6 months of age, the number of TH$^+$ immunoreactive neurons was similar between HIV-1 Tg and F344 rats (Fig. 2a). Representative images of TH immunohistochemistry in the SN showed a normal dense staining in neuronal cell bodies and processes of the SN at both 8 and 5 months (Fig. 2b, c). In HIV-1 Tg rats, TH immunoreactivity within neuronal cell bodies and processes was diminished at 8 months (Fig. 2b) but not at 5 months (Fig. 2c).

GFAP and Iba-1 Immunohistochemistry in the SN and Striatum

Microglia rapidly responds to changes that occur in neurons in close proximity and with synaptic damage and remodeling. Given the question of whether changes in glia might serve as an early indicator of neuronal alterations in the SN, we examined morphological changes in the SN and the striatum of rats at 5 months of age as representative of a time prior to pronounced changes in TH immunoreactivity in the SN. In the SN, Iba-1$^+$ microglia and GFAP$^+$ astrocytes showed a normal distribution and morphology (Fig. 2c; Supplementary Fig. 1). In the striatum, GFAP$^+$ astrocytes showed similar morphology across groups (Fig. 3). In F344 rats, Iba-1$^+$ cells (Fig. 3) were characterized by small cell bodies and long, thin processes. As compared with F344 rats, immunostaining for Iba-1 revealed a slight change in microglia in HIV-1 Tg rats. The visual appearance of a slightly more pronounced microglia morphology was supported by morphometric measurements in 70% ± 10% of the microglia showing slightly larger (10% ± 5%) cell

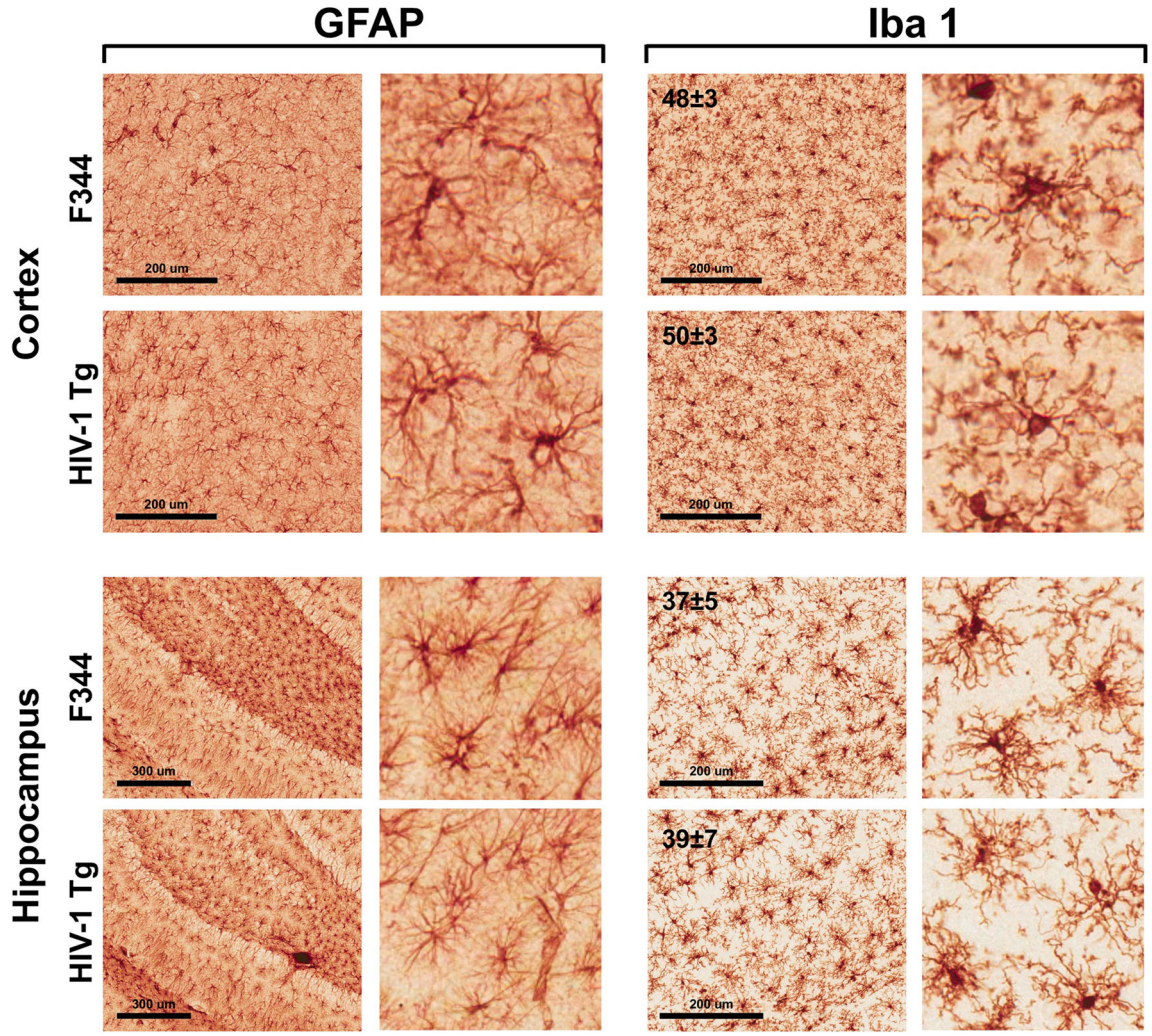

Fig. 4 Immunoreactivity for GFAP and Iba-1. Representative images of GFAP$^+$ astrocytes and Iba-1$^+$ microglia in the cortex and hippocampus of 5-month-old male F344 and HIV-1 Tg rats. 3,3-Diaminobenzidine (brown)-stained cells displayed normal process-bearing morphologies with no evidence of microglia activation or astrocyte hypertrophy. Quantitation of the % area occupied by Iba-1$^+$ immunoreactive cells (mean ± SD) in the cortex ($n = 6$) and hippocampus ($n = 10$) is provided within each representative image

bodies and thickened proximal processes (30% ± 8% ($t = 5.8$; $p < 0.01$) within a defined ROI.

Astrocyte and Microglia Morphology in the Hippocampus and Cortex

Previous studies have reported conflicting findings with regard to measures of astrocyte or microglia in the hippocampus or cortex of the HIV-1 Tg rat (Table 1). GFAP staining of astrocytes has been reported as either increased (Repunte-Canonigo et al. 2014) or decreased (Reid et al. 2016a). In the current study, a relatively uniform staining intensity and morphological distribution were observed for GFAP$^+$ astrocytes in both regions with no differences observed between F344 and HIV-1 Tg rats at 5 months (Fig. 4). Astrocytes maintained a normal cell body with thin processes and showed no evidence of hypertrophy. A similar pattern of conflicting results has been reported for microglia. Previous reports indicated that HIV-1 Tg rats showed no difference in microglia number in the cortex or hippocampus but an increase in microglia arborization (Repunte-Canonigo et al. 2014), number (Rowson et al. 2016), or no changes (Lee et al. 2015). In the current study, DAB-stained sections were examined for comparison with the literature and revealed a robust staining of microglia with no morphological differences observed in the HIV-1 Tg rats at 5 months of age (Fig. 4). Fluorescent staining

Fig. 5 mRNA levels for inflammatory genes in 5-month-old F344 and HIV-1 Tg male rats. **a** Substantia nigra (SN). **b** Striatum. **c** Cortex. **d** Hippocampus. mRNA levels were determined by qRT-PCR and normalized to cyclophilin in each sample. Data was calculated by $2^{r\Delta\Delta CT}$ presented as mean fold change in 5-month-old HIV-1 Tg male rats as compared with age-matched F344 rats ± SEM ($n = 4$). $^*p < 0.05$; $^{**}p < 0.01$

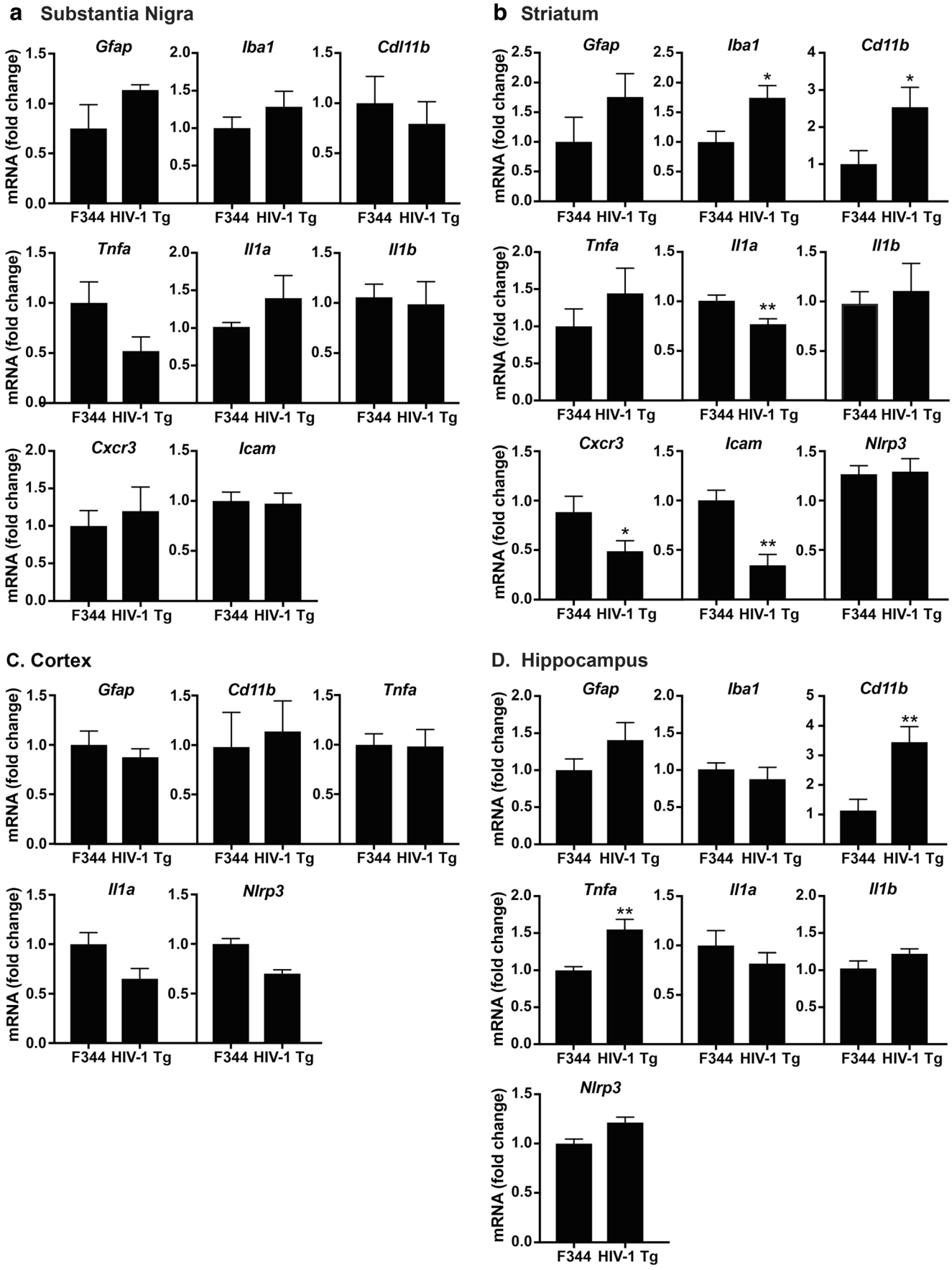
a Substantia Nigra
Gfap
Iba1
Cdl11b
Tnfa
Il1a
Il1b
Cxcr3
Icam
b Striatum
Gfap
Iba1
Cd11b
Tnfa
Il1a
Il1b
Cxcr3
Icam
Nlrp3
C. Cortex
Gfap
Cd11b
Tnfa
Il1a
Nlrp3
D. Hippocampus
Gfap
Iba1
Cd11b
Tnfa
Il1a
Il1b
Nlrp3
mRNA (fold change)
F344 HIV-1 Tg

showed similar results (Supplementary Fig. 2; Supplementary Fig. 3). Iba-1$^+$ microglia retained normal morphology characterized by a small cell body and fine ramified processes. No morphological evidence of microglia hypertrophy or of differentiation into an amoeboid phagocytic phenotype was observed. The total surface area occupied by Iba-1 immunoreactivity as calculated within multiple defined ROIs in the cortex and hippocampus showed no significant differences in HIV-1 Tg rats, as compared with F344 (Fig. 4).

mRNA Levels for Inflammatory Factors

The published literature is inconclusive with regard to evidence of an inflammatory response occurring in the brain of HIV1-Tg rats. Much of this appears to be related to the method of analysis, the age of analysis, and the region examined (Table 1) and could possibly be associated with a phenotypic drift in the rats over time. We focused our analysis on changes in inflammatory markers that occurred at 5 months of age, prior to the occurrence of diminished TH immunoreactivity in the SN and within an age range for an association to neurobehavioral alterations. As a comparison with previous published reports, multiple regions were examined including the striatum, SN, cortex, and hippocampus.

Substantia Nigra and Striatum The absence of overt morphological changes in astrocytes in the SN and striatum was supported by absence of differences in GFAP (Fig. 5a,b). In the SN, *Iba1*, *Cdllb*, *Tnfa*, *Il1a*, *Il1b*, C-X-C motif chemokine receptor 3 (*Cxcr3*), and intracellular adhesion molecule (*Icam*) mRNA levels were not significantly different in HIV-1 Tg rats as compared with F344 rats (Fig. 5a). In the striatum, the subtle morphological change in microglia morphology in the HIV-1 Tg rat was accompanied by a significant elevation in mRNA levels for *Iba1* ($t = 2.719$, $p < 0.05$). HIV-1 Tg rats showed significantly elevated mRNA levels for *Cdllb* ($t = 2.378$, df = 6, $p < 0.05$) and significantly lower mRNA levels for *Il1a* ($t = 3.022$, df = 6, $p < 0.05$) and *Icam* ($t = 4.322$, df = 6, $p < 0.01$; $p < 0.02$ corrected). The elevation in *Cxcr3* was no longer statistically significant following multiple comparison corrections ($t = 2.07$, df = 6, $p < 0.05$; $p < 1.0$ corrected). No differences were observed in mRNA levels for *Tnfa*, *Il1b*, or the inflammasome-related NLR family pyrin domain-containing 3 (*Nlrp3*) (Fig. 5b). Differences were not observed at 2 months of age (Supplementary Fig. 4).

The Cortex and Hippocampus Previous reports of immunohistochemical changes in GFAP astrocytes were accompanied by an increase in GFAP mRNA levels in the hippocampus but not in the cortex (Repunte-Canonigo et al. 2014) or with no changes in GFAP mRNA levels in the hippocampus even with substantially diminished GFAP staining intensity (Reid et al. 2016a). In the current study, consistent with the absence of immunohistochemical changes, mRNA levels for *Gfap* and *Iba-1* in the hippocampus and cortex were not significantly different in the HIV-1 Tg rat as compared with the F344 controls (Fig. 5c,d). In the cortex, mRNA levels for *Tnfa*, *Il1a*, and *Nlrp3* were not significantly altered in HIV-1 Tg rats as compared with F344 rats (Fig. 5c). In the hippocampus, mRNA levels for *Il1a*, *Il1b*, or *Nlrp3* were not altered; however, increases were observed for *Cd11b* ($t = 3.504$, df = 6, $p < 0.01$; $p < 0.02$ corrected) and *Tnfa* ($t = 3.77$, df = 6, $p < 0.01$; $p < 0.02$ corrected; Fig. 5d).

Discussion

In the human population, the association of neuroinflammation with the progression of HAND has a strong support both in the pre- and post-cART eras (review, Hong and Banks 2015). An age-dependent scenario has been proposed that involves alterations in neurotrophic factors (Bachis et al. 2016) or normal microglia function (DeVaughn et al. 2015) that can influence synaptic strength and remodeling. An involvement of dopaminergic system disruption appears to have strong supporting data, but at what stage a contribution of inflammatory factors might come into play cannot be adequately evaluated by the current conflicting literature. Using the HIV-1 Tg rat as a model, we report an age-related loss of TH$^+$ immunoreactivity in the SN that supports the various reports of an alteration in dopaminergic integrity. Microglia and astrocytes rapidly respond to changes in their environment, and we observed subtle changes in microglia morphology within the terminal dopaminergic synaptic field in the striatum. The thickening of the proximal process is consistent with a responsive action of microglia, and given the location as well as absence of mRNA elevations in various proinflammatory cytokines may be primarily indicative of early TH neuronal stress or dysfunction rather than cell death. No glial-related changes were noted in the cortex and only subtle elevations in *Cd11b* and *Tnfa* mRNA levels in the hippocampus, somewhat diminishing the hypothesis that behavioral changes were related to a neuroinflammatory process.

Even in the cART era, HIV-1-positive individuals display symptoms of cognitive impairment, some of which associate subcortical and frontal-striatal pathways (Becker et al. 2011). The utility of the HIV-1 Tg rat in assessing neurobehavioral functions has been well established with a large number of the studies conducted in animals between the ages of 2 and 6 months. One primary endpoint reported for HIV-1 Tg rats is a deficit in rotarod performance (June et al. 2009; Reid et al. 2016b). Our data is consistent with these findings in that HIV-1 Tg rats showed poorer performance at young ages; however, over a session, performance improved in both groups

suggesting effective learning of the task. This conclusion is somewhat in disagreement with that of Reid et al. (2016b) where performance was compared across weeks, and the authors concluded that the animals failed to habituate to the task given that the 60% decrease in latency did not reach statistical significance. The Reid et al. (2016b) study and the current study demonstrated that rotarod performance diminished with age such that, by the adult ages, it became difficult to discriminate between poorer motor performance and learning. Motor activity data have also been somewhat conflicting in HIV-1 Tg rats. Previous work reported no difference in motor activity over a 10-min session in 2-month-old HIV-1 Tg rats (Nemeth et al. 2014), while adult rats showed lower ambulatory and rearing activity over a 20-min test session (June et al. 2009). In comparison, in adult rats, we found no differences in ambulatory activity over a 30-min test session or at shorter intervals. Acclimation to a novel environment, such as an activity arena, can represent learning as well as response to stress. In adult male HIV-1 Tg rats, we did not observe activity patterns that would indicate an anxiety response in a novel environment. Additional assessments of learning and memory have utilized a modified Morris water maze (MWM) adjusted for cataract-related visual deficits in the HIV-1 Tg rat. Vigorito et al. (2007, 2013) reported acquisition of the task and thus, learning, in 5-month-old HIV-1 Tg rats; however, longer latencies were observed during the acquisition phase without a clear deficit in swim speed. In the probe test for memory, all rats displayed a similar preference for the escape quadrant suggesting equivalent learning and memory. Lashomb et al. (2009) expanded on this work and confirmed the ability of HIV-1 rats to learn the MWM; however, impairments were noted in search strategies that may involve the striatum circuitry (Packard and White 1991). The authors speculated that these outcomes were mediated by the D2 dopamine pathway of the basal ganglia, hippocampus, and cortex given the prolonged escape latencies without decreased swim speed (Stuchlik et al. 2007). Using tasks not as dependent on latency, Nesil et al. (2015) reported deficits in working memory in a spontaneous alternation maze paradigm, exploration, and memory in a novel object recognition task, in a step-through passive avoidance task in 2-month-old HIV-1 Tg rats. In the current study, we relied on an active avoidance procedure and found that HIV-1 Tg rats displayed a longer latency for the avoidance response and less number of avoidance responses; however, performance improved across the session. It is possible that such deficits in latency were related to changes in the dopaminergic pathway. The increased performance observed with training suggested basic learning capabilities in the HIV-1 Tg rats, but in the retest 6 weeks later, performance-suggested memory of the task may not be as well formed. While this behavior was evident prior to changes in TH immunoreactivity in the SN, it may still be related to an alteration in the dopaminergic pathway similar to that proposed for the MWM. It is possible that aging or a pharmacological challenge may unmask early alterations in dopaminergic-dependent behaviors and identify a greater level of compromised function in the HIV-1 Tg rat.

In the experimental models of HIV, pathology and dysfunction of the dopaminergic system have been reported (Bansal et al. 2000; Gelman et al. 2006; Silvers et al. 2006; Webb et al. 2010; Li et al. 2013; Reid et al. 2016a, b; Gaskill et al. 2017). In HIV-1 Tg rats, a dysregulation of the dopaminergic system has been suggested by molecular profiles related to alteration of DA transmission and Parkinson's disease (Repunte-Canonigo et al. 2014), a slight elevation in [18F]DPA-714] uptake (Lee et al. 2015), and decreased TH staining intensity in the striatum (Reid et al. 2016b). PET imaging of [18F]-fallypride striatal binding in aged HIV-1 Tg rats suggested a progressive degeneration of the DA system and decreased dopaminergic synaptic function in the striatum (Sinharay et al. 2017). Similar to the current findings, Miller et al. (2018) reported diminished TH immunostaining in the SN in GT-tg bigenic mice expressing HIV-1 Tat under GFAP. This occurred with reduced firing activity of DA neurons in the absence of neuronal death. While these deficits are observed in adult animals, it is also likely that subtle differences in the circuitry are present at younger ages. The work of Casas et al. (2017) suggested an effect of diminished volume and growth rate of the striatum between 5 and 9 weeks of age in HIV-1 Tg rats. This maturation pattern was functionally associated with rotarod performance. In the current study, the early performance deficits observed on the rotarod may reflect early alterations in the nigrostriatal network as impairment of the striatum can lead to motor coordination issues (Massaquoi and Hallett 1998).

It is thought that HIV viral products such as gp120, Tat, nef, and vif may promote ongoing inflammation and possible degeneration (Gannon et al. 2011; Zayyad and Spudich 2015). A subset of mononuclear phagocytes and astrocytes in HAND patients have been implicated as the source of proinflammatory cytokines and other neurotoxic molecules that may exacerbate damage to surrounding cells (Yadav and Collman 2009). How this translates to the rodent models is not as clear given the conflicting findings of glial response and cytokine elevation (Table 1). For example, astrocyte and microglia number was increased in the hippocampus and the cortex of 5-month old HIV-1 Tg rats, yet mRNA levels for *Gfap*, *Iba1*, and *Cd11b* were elevated only in the hippocampus (Repunte-Canonigo et al. 2014). With a detailed evaluation of microglia morphology in the hippocampus of young female rats, Rowson et al. (2016) reported no difference in number or average branch length but an increase in branch number, maximum length, and junctions. This was accompanied by a slight elevation in mRNA levels for complement factor b with no change in Lcn2. There was no indication of hypertrophy or cells differentiating to an amoeboid phenotype. Thus, a

relationship of microglia morphology to an inflammatory response is not established. Given the maturation pattern of microglia morphology, the enhanced arborization in the HIV-1 Tg rats may be reflective of differences manifesting during development. Using microPET imaging for TSPO, Lee et al. (2015) reported no differences in Iba-1$^+$ microglia cell density in HIV-1 Tg rats up to 9 months of age with no elevations in mRNA levels for proinflammatory cytokines in samples containing the striatum, cortex, and hippocampus. Reid et al. (2016a) reported diminished GFAP staining intensity in the striatum with no changes in microglia, similar to findings of a recent study by Sinharay et al. (2017) showing no differences in Iba-1$^+$ microglia but significantly lower GFAP staining of astrocytes as early as 1 month of age, extending until 18 months of age. Thus, overall the literature does not provide a solid representation of a neuroinflammatory state in the HIV-1 Tg rat brain that would account for the neurobehavioral differences reported. In general, these studies have relied on commonly analyzed components of neuroinflammation and do not exclude the possible involvement of other inflammatory processes such as lipid mediators. For example, Blanchard et al. (2015) reported elevations in whole brain prostaglandin E2, 15-epi-lipoxinA4, and 8-isoprostane in 9-month-old HIV-1 Tg rats while Repunte-Canonigo et al. (2014) reported an elevation in hippocampal mRNA levels for prostaglandin D2 at 5 months of age. It is possible that changes associated with neuroinflammation follow an age-dependent path with greater differences observed with increasing age. When older (18 months) HIV-1 Tg rats were examined, IL-1β and IL-6 levels were elevated in the striatum (Chivero et al. 2017). The elevation in Asc (apoptosis-associated speck-like protein containing a caspase recruitment domain) protein suggested an inflammatory component and possible activation of the inflammasome as a regulatory mechanism (Chivero et al. 2017), possibly as a direct activation of microglia (Walsh et al. 2014; Mamik et al. 2017). With the advanced age, it was not clear if the source of the inflammatory cytokines was related to resident microglia or the result of peripheral monocytes infiltration through a permeable blood-brain barrier as reported in Tat-expressing transgenic mice (Leibrand et al. 2017). Thus, differences observed for neuroinflammatory factors as a function of age may reflect the progressive damage to barrier integrity and raise a concern for a contribution of peripherally derived inflammatory factors in disease progression.

The current study provides a structural correlation to previous reports of alterations in the dopaminergic system. The data suggests that age-related loss of TH immunoreactivity in the SN contributed to earlier changes in the striatum. It remains to be determined if the subtle microglia hypertrophy in the striatum represented a response to changes in the terminal endings of the projecting TH$^+$ neurons (Schier et al. 2017). The current work was conducted in male rats, and, given the differential sensitivity of the female HIV-1 Tg rat to DA changes (McLaurin et al. 2017), the relationship between TH immunoreactivity in the SN and microglia changes in the striatum may occur earlier or be more pronounced in females. However, gender was not found to correlate with a decrease in DA levels observed in HIV-1 patients (Kumar et al. 2009), and the recent work by McLaurin et al. (2018) suggested that sex-related differences in motor activity and acoustic startle response were not observed across the adult ages examined in the current study. There was a difference in prepulse startle inhibition. Thus, we feel that examining only one sex does not diminish the characteristics described but does open the possibility for examining sex-related differences in future studies. Alternatively, responses may be associated with an accumulation of viral-related proteins that occur in the striatum between 2 and 10 months of age (Peng et al. 2010). A direct cortical injection of HIV-1 Tat1–72 was associated with microglial contacts with multiple nondegenerating neuronal components within as early as 24 h (Marker et al. 2013). It was suggested that cell-cell contacts mediated by microglial filopodia may function in a preliminary step in the elimination of synaptic structures. While it is often expected that microglia activation is associated with an upregulation of proinflammatory factors, this may not necessarily occur with microglial phagocytosis that occurs in response to apoptotic cellular material. In this case, activation of such receptors that recognize phosphatidylserine (PS) stimulates an antiinflammatory response in phagocytes (Ravichandran 2003). The observation of a subtle microglia morphological response and lower *Il1a* level with no change in *Tnfa* in the striatum may be related to synaptic phagocytic activity of microglia. Cxcr3 functions to recruit microglia to a site of injury (Rappert et al. 2004), and thus, lower levels of *Cxcr3* and *Icam* may serve to minimize recruitment as a regulatory mechanism in this early stage of cellular insult. These findings raise questions for future studies to determine if this represents a tightly regulated response to minimize cell activation to the neuronal insult or a dysregulated microglia response. Given the findings of an age-related change in TH immunoreactivity in the SN from the current study and in the striatum (Reid et al. 2016a), additional behavioral tests and pharmacological challenges can now be incorporated into future studies to examine the long-term implications of these anatomical findings.

Funding Information This work was supported in part by HHS grants NS079172 and NS074916 to IM and NIH intramural research funding Z01 ES021164-12 and Z01 ES101623-05 to JH.

Compliance with Ethical Standards Animal studies were done in accordance with the National Institutes of Health *Guide for the Care and Use of Laboratory Animals* following approved animal

protocols from the Animal Care and Use Committee of the National Institute of Environmental Health Sciences.

Conflict of Interest The authors declare that they have no conflict of interest.

References

Atluri VS, Kanthikeel SP, Reddy PV, Yndart A, Nair MP (2013) Human synaptic plasticity gene expression profile and dendritic spine density changes in HIV-infected human CNS cells: role in HIV-associated neurocognitive disorders (HAND). PLoS One 8: e61399. https://doi.org/10.1371/journal.pone.0061399

Avdoshina V, Fields JA, Castellano P, Dedoni S, Palchik G, Trejo M, Adame A, Rockenstein E, Eugenin E, Masliah E, Mocchetti I (2016) The HIV Protein gp120 Alters Mitochondrial Dynamics in Neurons. Neurotox Res 29 (4):583-593

Avdoshina V, Caragher SP, Wenzel ED, Taraballi F, Moccchetti I, Harry GJ (2017) The viral protein gp120 decreases the acetylation of neuronal tubulin: potential mechanism of neurotoxicity. J Neurochem 141:606–613

Bachis A, Wenzel E, Boelk A, Becker J, Mocchetti I (2016) The neurotrophin receptor p75 mediates gp120-induced loss of synaptic spines in aging mice. Neurobiol Aging 46:160–168

Bansal AK, Mactutus CF, Nath A, Maragos W, Hauser KF, Booze RM (2000) Neurotoxicity of HIV-1 proteins gp120 and Tat in the rat striatum. Brain Res 879:42–49

Blanchard HC, Taha AY, Rapoport SI, Yuan Z-X (2015) Low-dose aspirin (acetylsalicylate) prevents increases in brain PGE_2, 15-epi-lipoxin A4 and 8-isoprostane concentrations in 9 month-old HIV-1 transgenic rats, a model for HIV-1 associated neurocognitive disorders. Prostaglandins Leukot Essent Fat Acids 96:25–30

Berger JR, Kumar M, Kumar A, Fernandez JB, Levin B (1994) Cerebrospinal fluid dopamine in HIV-1 infection. AIDS 8:67-71

Bertrand SJ, Mactutus CF, Harrod SB, Moran LM, Booze RM (2018) HIV-1 proteins dysregulate motivational processes and dopamine circuitry. Sci Rep 8:7869

Boban J, Kozic D, Turkulov V, Ostojic J, Semnic R, Lendak D, Brkic S (2017) HIV-associated neurodegeneration and neuroimmunity: multivoxel MR spectroscopy study in drug-naïve and treated patients. Eur Radiol 27:4218–4236

Casas R, Muthusamy S, Wakim PG, Sinharay S, Lentz MR, Reid WC, Hammoud DA (2017) MR brain volumetric measurements are predictive of neurobehavioral impairment in the HIV-1 transgenic rat. NeuroImge Clin 17:659–666

Chan P, Hellmuth J, Spudich S, Valcour V (2016) Cognitive impairment and persistent CNS injury in treated CNS. Curr HIV/AIDS Rep 13: 209–217. https://doi.org/10.1007/s11904-016-0319-7

Chen MF, Gill AJ, Kolson DL (2014) Neuropathogenesis of HIV-associated neurocognitive disorders: roles for immune activation, HIV blipping and viral tropism. Curr Opin HIV AIDS 9:559-564

Chivero ET, Guo M-L, Periyasamy P, Liao K, Callen SE, Buch S (2017) HIV-1 Tat primes and activates microglial NLRP3 inflammasome-mediated neuroinflammation. J Neurosci 37:3599–3609

Cho Y-E, Lee M-H, Song B-J (2017) Neuronal cell death and degeneration through increased nitroxidative stress and tau phosphorylation in HIV-1 transgenic rats. PLoS One 12(1):e0169945

Clifford KM, Samboju V, Cobigo Y, Milanini B, Marx GA, Hellmuth JM, Rosen HJ, Kramer JH, Allen IE, Valcour VG (2017) Progressive brain atrophy despite persistent viral suppression in HIV over age 60. J Acquir Immune Defic Syndr 76:289–297

DeVaughn S, Müller-Oehring EM, Markey B, Brontë-Stewart HM, Schulte T (2015) Aging with HIV-1 infection: motor functions, cognition, and attention – a comparison with Parkinson's Disease. Neuropsychol Rev 25:424–438

Gannon P, Khan MZ, Kolson DL (2011) Current understanding of HIV-associated neurocognitive disorders pathogenesis. Curr Opin Neurol 24:275–283. https://doi.org/10.1097/WCO.0b013e32834695fb

Gaskill PJ, Carvallo L, Eugenin EA, Berman JW (2012) Characterization and function of the human macrophage dopaminergic system: implications for CNS disease and drug abuse. J Neuroinflammation 9: 203. https://doi.org/10.1186/1742-2094-9-203

Gaskill PJ, Calderon TM, Coley JS, Berman JW (2013) Drug induced increases in CNS dopamine alter monocyte, macrophage and T cell functions: implications for HAND. J NeuroImmune Pharmacol 8: 621–642

Gaskill PJ, Yano HH, Kalpana GV, Javitch JA, Berman JW (2014) Dopamine receptor activation increases HIV entry into primary human macrophages. PLoS One 9:e108232

Gaskill PJ, Miller DR, Gamble-George J, Yano H, Khoshbouei H (2017) HIV, Tat and dopamine transmission. Neurobiol Dis 105:51–73

Gelman BB (2015) Neuropathology of HAND with suppressive antiretroviral therapy: encephalitis and neurodegeneration reconsidered. Curr HIV/AIDS Rep 12:272–279

Gelman BB, Spencer JA, Holzer CE III, Soukup VM (2006) Abnormal striatal dopaminergic synapses in national NeuroAIDS tissue consortium subjects with HIV encephalitis. J NeuroImmune Pharmacol 1:410–420

Ginsberg SD, Alldred MJ, Sunnam SM, Schiroli C, Lee SH, Morgello S, Fischer T (2018) Expression profiling suggests microglial impairment in human immunodeficiency virus neuropathogenesis. Ann Neurol 83:206–417

Gundersen HJG, Jensen EBV, Kieu K, Nielsen J (1999) The efficiency of systematic sampling in stereology - reconsidered. J Micros 193(3): 199-211

Guo M, Bryant J, Sultana S, Jones O, Royal W III, (2012) Effects of vitamin A deficiency and opioids on parvalbumin+ interneurons in the hippocampus of the HIV-1 transgenic rat. Curr HIV Res 10(5): 463-468

Harry GJ, Hooth MJ, Vallant M, Behl M, Travlos GS, Howard JL, Price CJ, McBride S, Mervis R, Mouton PR (2014) Developmental neurotoxicity of 3,3′,4,4′-tetrachloroazobenzene with thyroxine deficit: sensitivity of glia and dentate granule neurons in the absence of behavioral changes. Toxics 3:496–532

Heaton RK, Clifford DB, Franklin DR Jr, Woods SP, Ake C, Vaida F, Ellis RJ, Letendre SL, Marcotte TD, Atkinson JH, Rivera-Mindt M, Vigil OR, Taylor MJ, Collier AC, Marra CM, Gelman BB, McArthur JC, Morgello S, Simpson DM, McCutchan JA, Abramson I, Gamst A, Fennema-Notestine C, Jernigan TL, Wong J, Grant I, For the CHARTER Group (2010) HIV-associated neurocognitive disorders persist in the era of potent antiretroviral therapy: CHARTER Study. Neurology 75:2087–2096

Heppner FL, Roth K, Nitsch R, Hailer NP (1998) Vitamin E induces ramification and downregulation of adhesion molecules in cultured microglial cells. Glia 22:180–188

Hong S, Banks WA (2015) Role of the immune system in HIV-associated neuroinflammation and neurocognitive implications. Brain Behav Immun 45:1–12

Hu S, Sheng WS, Lokensgard JR, Peterson PK, Rock RB (2009) Preferential sensitivity of human dopaminergic neurons to gp120-induced oxidative damage. J Neurovirol 15:401–410

Itoh K, Mehraein P, Weis S (2000) Neuronal damage of the substantia nigra in HIV-1 infected brains. Acta Neuropathol 99:376–384

Javadi-Paydar M, Roscoe RF Jr, Denton AR, Mactutus CF, Booze RM (2017) HIV-1 and cocaine disrupt dopamine reuptake and medium spiny neurons in female rat striatum. PLoS One 12(11):e0188404. https://doi.org/10.1371/journal.pone.0188404

June HL, Yang ARST, Bryant JL, Jones O, Royal W (2009) Vitamin A deficiency and behavioral and motor deficits in the HIV-1 transgenic rat. J Neurovirol 15:380–389

Kanaan NM, Kordower JH, Collier TJ (2008) Age and region-specific responses of microglia, but not astrocytes, suggest a role in selective vulnerability of dopamine neurons after 1-methyl-4-phenyl-1,2,3,6-tetrahydropyridine exposure in monkeys. Glia 56:1199–1214

Kieburtz KD, Epstein LG, Gelbard HA, Greenamyre JT (1991) Excitotoxicity and dopaminergic dysfunction in the acquired immunodeficiency syndrome dementia complex. Therapeutic implications. Arch Neurol 48:1281–1284

Kim HJ, Shin AH, Thayer SA (2011) Activation of cannabinoid type 2 receptors inhibits HIV-1 envelope glycoprotein gp 120-induced synapse loss. Mol Pharmacol 80:357–366

Kumar AM, Fernandez JB, Singer EJ, Commins D, Waldrop-Valverde D, Ownby RL, Kumar M (2009) Human immunodeficiency virus type 1 in the central nervous system leads to decreased dopamine in different regions of postmortem human brains. J Neuro-Oncol 15: 257–274

Lashomb AL, Vigorito M, Chang SL (2009) Further characterization of the spatial learning deficit in the human immunodeficiency virus-1 transgenic rat. J Neuro-Oncol 15:14–24

Lassiter C, Fan X, Joshi PC, Jacob BA, Sutliff RL, Jones DP, Koval M, Guidot DM (2009) HIV-1 transgene expression in rats causes oxidant stress and alveolar epithelial barrier dysfunction. AIDS ResTher 6(1). https://doi.org/10.1186/1742-6405-6-1

Lee DE, Yue X, Ibrahim WG, Lentz MR, Peterson KL, Jagoda EM, Kassiou M, Maric D, Reid WC, Hammoud DA (2015) Lack of neuroinflammation in the HIV-1 transgenic rat: an [18F]-DPA714 PET imaging study. J Neuroinflammation 12:171. https://doi.org/10.1186/s12974-015-0390-9

Letendre SL, Ellis RJ, Ances BM, McCutchan JA (2010) Neurologic complications of HIV disease and their treatment. Top HIV Med 18:45–55

Levine AJ, Soontornniyomkij V, Achim CL, Masliah E, Gelman BB, Sinsheimer JS, Singer EJ, Moore DJ (2016) Multilevel analysis of neuropathogenesis of neurocognitive impairment in HIV. J Neuro-Oncol 22:431–441

Leibrand CR, Paris JJ, Ghandour MS, Knapp PE, Kim WK, Hauser KF, McRae M (2017) HIV-1 Tat disrupts blood-brain barrier integrity and increases phagocytic perivascular macrophages and microglia in the dorsal striatum of transgenic mice. Neurosci Lett 640:136–143

Li MD, Cao J, Wang S, Wang J, Sarkar S, Vigorito M, Ma JZ, Chang SL (2013) Transcriptome sequencing of gene expression in the brain of the HIV-1 transgenic rat. PLoS One. https://doi.org/10.1371/journal.pone.0059582

Liu X, Chang L, Vigorito M, Kass M, Li H, Chang SL (2009) Methamphetamine-induced behavioral sensitization is enhanced in the HIV-1 transgenic rat. J NeuroImmune Pharmacol 4(3):309–316

Lopez OL, Smith G, Meltzer CC, Becker JT (1999) Dopamine systems in human immunodeficiency virus-associated dementia. Neuropsychiatry Neuropsychol Behav Neurol 12:184–192

Mamik MK, Hui E, Branton WG, McKenzie BA, Chisholm J, Cohen EA, Power C (2017) HIV-1 viral protein R activates NLRP3 inflammasome in microglia: implications for HIV-1 associated neuroinflammation. J NeuroImmune Pharmacol 12:233–248

Marcario JK, Manaye KF, Santacruz KS, Mouton PR, Berman NEJ, Cheney PD (2004) Severe subcortical degeneration in macaques infected with neurovirulent simian immunodeficiency virus. J Neurovirol 10:1–13

Marker DF, Tremblay M-E, Puccini JM, Barbieri J, Gantz-Maarker MA, Loweth CJ, Muly C, Lu S-M, Goodfellow VS, Dewhurst S, Gelbard HA (2013) The new small-molecule mixed-lineage kinase 3 inhibitor URMC-099 is neuroprotective and anti-inflammatory in models of human immunodeficiency virus-associated neurocognitive disorders. J Neurosci 33:9998–10010

Massaquoi SG, Hallett M (1998) Ataxia and other cerebellar syndromes. In: Jankovic J, Tolosa E (eds) Parkinson's disease and movement disorders. Williams & Wilkins, Baltimore

McArthur JC, Steiner J, Sacktor N, Nath A (2010) Human immunodeficiency virus-associated neurocognitive disorders: mind the gap. Ann Neurol 67:699–714

McIntosh S, Sexton T, Pattison LP, Childers SR, Hemby SE (2015) Increased sensitivity to cocaine self-administration in HIV-1 transgenic rats is associated with changes in striatal dopamine transporter binding. J NeuroImmune Pharmacol 10:493–505

McLaurin KA, Booze RM, Mactutus CF, Fairchild AJ (2017) Sex matters: robust sex differences in signal detection in the HIV-1 transgenic rat. Front Behav Neurosci 11:212. https://doi.org/10.3389/fnbeh.2017.00212

McLaurin KA, Booze RM, Mactutus CF (2018) Evolution of the HIV-1 transgenic rat: utility in assessing the progression of HIV-1 associated neurocognitive disorders. J Neurovirol 24:229–245

Miller DR, Shaerzadeh F, Phan L, Sharif, Gamble-George J, McLaughlin JP, Streit WJ, Khoshbouei H (2018) HIV-1 Tat regulation of dopamine transmission and microglial reactivity is brain region specific. Glia. https://doi.org/10.1002/glia.23447

Moran LM, Booze RM, Webb KM, Mactutus CF (2013) Neurobehavioral alterations in HIV-1 transgenic rats: evidence for dopaminergic dysfunction. Exp Neurol 239:139–147

Moscarello JM, LeDoux JE (2013) Active avoidance learning requires prefrontal suppression of amygdala-mediated defensive reactions. J Neurosci 33:3815–3823

Mouton PR, Gokhale AM, Ward NL, West MJ (2002) Stereological length estimation using spherical probes. J Microsc 206(1):54-64

Mouton PR, Gordon M (2010) Stereological and image analysis techniques for quantitative assessment of neurotoxicology. In: Neurotoxicology, 3rd ed. Ed: GJ Harry, H.A. Tilson, London: Informa Press

Nemeth CL, Glasper ER, Harrell CS, Malviya SA, Otis JS, Neigh GN (2014) Meloxicam blocks neuroinflammation, but not depressive-like behaviors, in HIV-1 transgenic female rats. PLoS One 9(10): e108399

Nesil T, Cao J, Yang Z, Chang SL, Li MD (2015) Nicotine attenuates the effect of HIV-1 proteins on the neural circuits of working and contextual memories. Mol Brain 8:43. https://doi.org/10.1186/s13041-015-0134-x

Nolan RA, Muir R, Runner K, Haddad EK, Gaskill PJ (2019) Pole of macrophage dopamine receptors in mediating cytokine production: implications for neuroinflammation in the context of HIV-associated neurocognitive disorders. J NeuroImmune Pharmacol 14:134–156

Nosheny RL, Bachis A, Aden SA, DeBernardi MA, Mocchetti I (2006) Intrastriatal administration of human immunodeficiency virus-1 glycoprotein 120 reduces glial cell-line derived neurotrophic factor levels and causes apoptosis in the substantia nigra. J Neurobiol 66: 1311–1321

NTP (National Toxicology Program) (2015) Neurobehavioral testing specifications. https://ntp.niehs.nih.gov/ntp/test_info/finalntp_neurospecs090415_508.pdf [accessed 06/14/2019]

Packard MG, White NM (1991) Dissociation of hippocampus and caudate nucleus memory systems by posttraining intracerebral injection of dopamine agonists. Behav Neurosci 105:295–306

Pang X, Panee J (2016) Anti-inflammatory function of *Phyllostachys edulis* extract in the hippocampus of HIV-1 transgenic mice. J HIV AIDS 2(3). https://doi.org/10.16966/2380-5536.126

Peng J, Vigorito M, Liu X, Zhou D, Wu X, Chang SL (2010) The HIV-1 transgenic rat as a model for HIV-1 infected individuals on HAART.

J Neuroimmunol 218:94–101
Ramirez F, Moscarello JM, LeDoux JE, Sears RM (2015) Active avoidance requires a serial basal amygdala to nucleus accumbens shell circuit. J Neurosci 35:3470–3477
Rao VR, Ruiz AP, Prasad VR (2014) Viral and cellular factors underlying neuropathogenesis in HIV associated neurocognitive disorders (HAND). AIDS Res Ther. https://doi.org/10.1186/1742-6405-11-13
Rappert A, Bechmann I, Pivneva T, Mahlo J, Biber K, Nolte C, Kovac AD, Gerard C, Boddeke HW, Nitsch R, Kettenmann H (2004) CXCR3-dependent microglial recruitment is essential for dendrite loss after brain lesion. J Neurosci 24:8500–8509
Ravichandran KS (2003) "Recruitment signals" from apoptotic cells: invitation to a quiet meal. Cell 113(7):817–820
Reid WC, Ibrahim WG, Kim SJ, Denaro F, Casas R, Lee DE, Maric D, Hammoud DA (2016a) Characterization of neuropathology in the HIV-1 transgenic rat at different ages. J Neuroimmunol 292:116–125
Reid WC, Casas R, Papadakis GZ, Muthusamy S, Lee DE, Ibrahim WG, Nair A, Koziol D, Maric D, Hammoud DA (2016b) Neurobehavioral abnormalities in the HIV-1 transgenic rat do not correspond to neuronal hypometabolism on ^{18}F-FDG-PET. PLoS One 11(3):e0152265. https://doi.org/10.1371/journal.pone.0152265
Reid W, Sadowska M, Denaro F, Rao S, Foulke J Jr, Hayes N, Jones O, Doodnauth D, Davis H, Sill A, O'Driscoll P, Huso D, Fouts T, Lewis G, Hill M, Kamin-Lewis R, Wei C, Ray P, Gallo RC, Reitz M, Bryant J (2001) An HIV-1 transgenic rat that develops HIV-related pathology and immunologic dysfunction. Proc Natl Acad Sci U S A 98(16):9271–9276
Repunte-Canonigo V, Lefebvre C, George O, Kawamura T, Morales M, Koob GF, Califano A, Masliah E, Sanna PP (2014) Gene expression changes consistent with neuroAIDS and impaired working memory in HIV-1 transgenic rats. Mol Neurodegener 9:26. https://doi.org/10.1186/1750-1326-9-26
Reyes MG, Faraldi F, Senseng S, Flowers C, Pariello R (1991) Nigral degeneration in acquired immune deficiency syndrome (AIDS). Acta Neuropathol 82:39–44
Roscoe RF Jr, Mactutus CF, Booze RM (2014) HIV-1 transgenic female rat: synaptodendritic alterations of medium spiny neurons in the nucleus accumbens. J NeuroImmune Pharmacol 9(5):642–653
Rowson SA, Harrell CS, Bekhbat M, Gangavelli A, Wu MJ, Kelly SD, Reddy R, Neigh GN (2016) Neuroinflammation and behavior in HIV-1 transgenic rats exposed to chronic adolescent stress. Front Psychiatry 7:102. https://doi.org/10.3389/fpsyt.2016.00102
Royal W III, Zhang L, Guo M, Jones O, David H, Bryant JL (2012) Immune activation, viral gene product expression and neurotoxicity in the HIV-1 transgenic rat. J Neuroimmunol 247:16–24
Rozzi SJ, Avdoshina V, Fields JA, Trejo M, Ton HT, Ahem GP, Mocchetti I (2017) Human immunodeficiency virus promotes mitochondrial toxicity. Neurotox Res 32:723–733
Ru W, Tang S-J (2017) HIV-associated synaptic degeneration. Mol Brain 10:40. https://doi.org/10.1186/s13041-017-0321-z
Sacktor N, Robertson K (2014) Evolving clinical phenotypes in HIV-associated neurocognitive disorders. Curr Opin HIV AIDS 9(6):517–520
Sanford R, Fellows LK, Ances BM, Collins DL (2018) Association of brain structure changes and cognitive function with combinational antiretroviral therapy in HIV-positive individuals. JAMA Neurol 75:72–79
Sanna PP, Repunte-Canonigo V, Masliah E, Lefebvre C (2017) Gene expression patterns associated with neurological disease in human HIV infection. PLoS One 12(4):e0175316. https://doi.org/10.1371/journal.pone.0175316
Saylor D, Dickens AM, Sacktor N, Haughey N, Slusher B, Pletnikov M, Mankowski JL, Brown A, Volsky DJ, McArthur JC (2016) HIV-associated neurocognitive disorder-pathogenesis and prospects for treatment. Nat Rev Neurol 12:234–248
Schier CJ, Marks WD, Paris JJ, Barbour AJ, McLane VD, Maragos WF, McQuiston AR, Knapp PE, Hauser KF (2017) Selective vulnerability of striatal D2 versus D1 dopamine receptor-expressing medium spiny neurons in HIV-1 Tat transgenic male mice. J Neurosci 37:5758–5769
Schouten J, Cinque P, Gisslen M, Reiss P, Portegies P (2011) HIV-1 infection and cognitive impairment in the cART era: a review. AIDS 25(5):561–575
Shin AH, Kim HJ, Thayer SA (2012) Subtype selective NMDA receptor antagonists induce recovery of synapses lost following exposure to HIV-1 Tat. Br J Pharmacol 166:1002–1017
Sheppard DP, Woods SP, Bondi MW, Gilbert PE, Massman PJ, Doyle KL, HIV Neurobehavioral Research Program (2015) Does older age confer an increased risk of incident neurocognitive disorders among persons living with HIV disease? Clin Neuropsychol 29:656–677
Silvers JM, Aksenov MY, Aksenova MV, Beckley J, Olton P, Mactutus CF, Booze RM (2006) Dopaminergic marker proteins in the substantia nigra of human immunodeficiency virus type 1-infected brains. J NeuroVirol 12:140–145
Sinharay S, Lee D, Shah S, Muthusamy S, Papadakis GZ, Zhang X, Maric D, Reid WC, Hammoud DA (2017) Cross-sectional and longitudinal small animal PET shows pre and post-synaptic striatal dopaminergic deficits in an animal model of HIV. Nucl Med Biol 55:27–33
Stuchlik A, Rehakova L, Telensky P, Vales K (2007) Morris water maze learning in Long-Evans rats is differentially affected by blockade of D1-like and D2-like dopamine receptors. Neurosci Lett 422:169–174
Theodore S, Cass WA, Dwoskin LP, Maragos WF (2012) HIV-1 protein Tat inhibits vesicular monamine transporter-2 activity in rat striatum. Synapse 66:755–757
Underwood J, Cole JH, Caan M, DeFrancesco D, Leech R, van Zoest RA, Su T, Geurtsen GJ, Schmand BA, Portegies P, Prins M, Wit FW, Sabin CA, Majoie C, Reiss P, Winston A, Sharp DJ (2017) Gray and white matter abnormalities in treated HIV-disease and their relationship to cognitive function. Clin Infect Dis 65:422–432
van den Dries LWJ, Wagener MN, Jiskoot LC, Visser M, Robertson KR, Adriani KS, van Gorp ECM (2017) Neurocognitive impairment in a chronically well-suppressed HIV-infected population: the Dutch TREVI cohort study. AIDS Patient Care STDs 31:329–334
Vera JH, Guo Q, Cole JH, Boasso A, Greathead L, Kelleher P, Rabiner EA, Kalk N, Bishop C, Gunn RN, Matthews PM, Winston A (2016) Neuroinflammation in treated HIV-positive individuals: a TSPO PET study. Neurology 86:1425–1432
Vigorito M, Lashomb AL, Chang SL (2007) Spatial learning and memory in HIV-1 transgenic rats. J NeuroImmune Pharmacol 2:319–328
Vigorito M, Cao J, Li MD, Chang SL (2013) Acquisition and long-term retention of spatial learning in the human immunodeficiency virus-1 transgenic rat: effects of repeated nicotine treatment. J Neuro-Oncol 19:157–165
Walsh JG, Reinke SN, Mamik MK, McKenzie BA, Maingat F, Branton WG, Broadhurst DI, Power C (2014) Rapid inflammasome activation in microglia contributes to brain disease in HIV/AIDS. Retrovirology 11:35. https://doi.org/10.1186/1742-4690-11-35
Wang GJ, Chang L, Volkow ND, Telang F, Logan J, Ernst T, Fowler JS (2004) Decreased brain dopaminergic transporters in HIV-associated dementia patients. Brain 127:2452–2458
Webb KM, Aksenov MY, Mactutus CF, Booze RM (2010) Evidence for developmental dopaminergic alterations in the human immunodeficiency virus-1 transgenic rat. J Neurovirol 16:168–173
Yadav A, Collman RG (2009) CNS inflammation and macrophage/microglial biology associated with HIV-1 infection. J

NeuroImmune Pharmacol 4:430–447

Yang Z, Nesil T, Connaghan KP, Li MD, Chang S (2016) Modulation effect of HIV-1 viral proteins and nicotine on expression of the immune-related genes in brain of the HIV-1 transgenic rats. J NeuroImmune Pharmacol 11:562–571

Zayyad Z, Spudich S (2015) Neuropathogenesis of HIV: from initial neuroinvasion to HIV-associated neurocognitive disorder (HAND). Curr HIV/AIDS Rep 12:16–24

Zhu J, Yuan Y, Midde NM, Gomez AM, Sun WL, Quizon PM, Zhan CG (2016) HIV-1 transgenic rats display and increase in ^{3}[H] dopamine uptake in the prefrontal cortex and striatum. J Neurovirol 22:282–292